ABSTRACT

Title of Thesis: BIO-DERIVED MICROSCALE CONTAINERS FOR DISEASE TREATMENT AND DIAGNOSTICS

James Yan Liu, Master of Science, 2017

Directed By: Professor Srinivasa R. Raghavan
Department of Chemical and Biomolecular Engineering

Micro-erythrosomes (mERs) are microscale containers (3 to 5 μm in diameter) derived from red blood cells (RBCs, also called erythrocytes). They are prepared by removing hemoglobin from RBCs and resuspending the empty structures in buffer. In this work, we focus on adding new functionalities to mERs, with both therapeutics and diagnostics in mind. In our main study, we demonstrate the use of mERs as "Killer Cells" to attack cancer. mERs are loaded with the enzyme glucose oxidase (GOx) and then incubated *in vitro* with a strain of head and neck cancer cells (15B). In the presence of glucose from external media, the Killer Cells generate hydrogen peroxide (H_2O_2). H_2O_2 is a reactive oxygen species (ROS) which induces the cancer cells to undergo apoptosis (programmed cell death). We find a reduction in 15B cell viability of over 80%. In ancillary studies, we explore strategies for the long-term retention of solutes in mERS. Specifically, the cationic biopolymer chitosan is adsorbed to the surfaces of mERs, and the anionic biopolymer alginate is encapsulated in their cores. Both strategies are able to extend the diffusion time for loaded solutes. Additionally, we have attempted to adapt mERs for use as MRI contrast agents by incorporating lipids containing gadolinium into the membrane. These studies lay the foundation for many mER applications and demonstrate their versatility.

BIO-DERIVED MICROSCALE CONTAINERS FOR DISEASE TREATMENT AND DIAGNOSTICS

By

James Y. Liu

Thesis submitted to the Faculty of the Graduate School of the
University of Maryland, College Park, in partial fulfillment
of the requirements for the degree of
Master of Science
2017

Advisory Committee:

Prof. Srinivasa R. Raghavan, Dept. of Chemical and Biomolecular Engineering
Prof. Jeffery B. Klauda, Dept. of Chemical and Biomolecular Engineering
Prof. Ganesh Sriram, Dept. of Chemical and Biomolecular Engineering

Acknowledgments

I would first like to thank my advisor, Dr. Srinivasa Raghavan, for his support and guidance throughout my research. He taught me how to transform my research into a coherent story, and pushed me to reach higher. I would like to thank my committee members, both for their service and their part as my teachers.

I would like to thank Dr. David Quan, of the Bentley lab, for his invaluable assistance with experiments involving cell culture. I would like to thank Amy Beaven, director of the Imaging Core, for assistance with confocal microscopy.

I would like to thank my fellow members of the Complex Fluids Group, Dr. Ankit Gargava, Dr. Brady Zarket, Kerry DeMella, Toniya Acharya, Niti Agrawal, Kurt Sweely, Dr. Matthew Dowling, SoHyun Ahn, Trip Fernandes, Michael Rudy, Hanchu Wang, and Chunxue Zhang for their assistance and good company during my stay. I would especially like to thank Dr. Charles Kuo, who mentored me when I first joined, laid the groundwork for my research direction, and was open to my questions even after moving on from the lab.

Finally, I would like to thank my family. They have always encouraged me to apply myself and realize my potential. Without their support, I would never have made it this far.

Table of Contents

List of Figures

Chapter 1

Introduction

1.1 Problem Description and Significance

The search for robust, biocompatible, and modifiable structures at the micro to nano size scale has been a major component of biomedical research. Many drugs, enzymes, etc. that are used to treat disease are unstable on their own, but could be successfully delivered systemically if they were encapsulated in such containers. Additionally, if one could enable these containers to selectively reach their target (a specific organ, a tumor, etc.), then the dose at that location would be higher, therefore effectiveness would be increased, and possible side effects would be reduced. This provides the motivation to design small structures that can carry a desired cargo.

Micro-erythrosomes (mERs) are microscale containers (3 to 5 μm) derived from red blood cells (RBCs). They retain many of the properties of the parent RBCs, such as their biocompatibility and long circulation time, giving them advantages over other microstructures. mERs have not been thoroughly studied in the literature, and therefore have much unexplored potential. This thesis focuses on the modification of mERs, with applications in both the therapeutic and diagnostic sides of medicine. We discuss passive improvements such as enhancing their release properties, as well as an active role in which they destroy cancer cells.

1.2 Proposed Approach

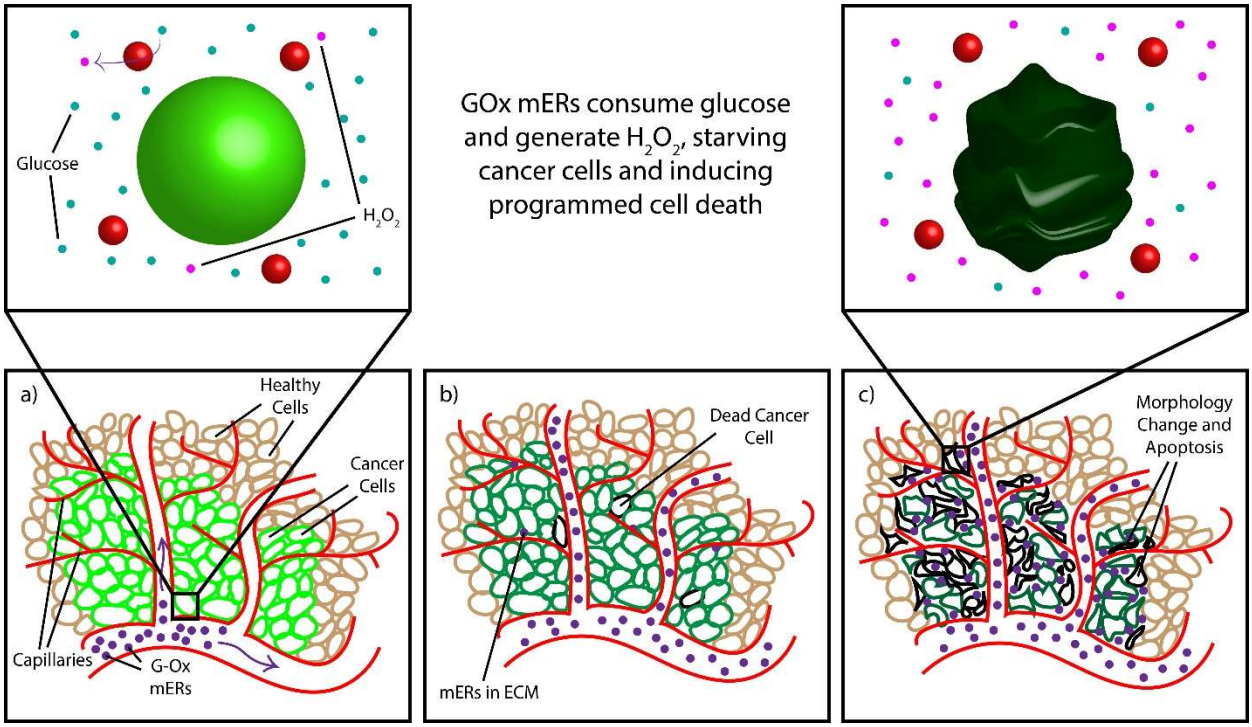

Figure 1.1. mERs as "Killer Cells"

In Chapter 3, we present the use of mERs as "Killer Cells" to attack cancer, as illustrated in Figure 1.1. Cancer is one of the most prolific and tenacious diseases, and existing treatments leave much to be desired. We propose a new approach for combating cancer where mERs are loaded with the enzyme glucose oxidase (GOx) and dispatched through the bloodstream. In the vicinity of the cancer cells, these mERs will convert glucose into hydrogen peroxide (H_2O_2), which is cytotoxic, and thereby induce cancer cell death. The body's own immune system serves as an inspiration for the concept, hence the term "Killer Cells." In our studies we conduct *in vitro* experiments with a cancer cell line and explore cell viability in the presence of varying concentrations of killer mERs. This work serves as an important proof-of-concept that may lead to more sophisticated mER therapies.

In Chapter 4, we examine three other applications of mERs. Two of them are motivated by the common goal of achieving slower (and thereby more extended) release of solutes from mERs. The ability of containers to release contents over a longer timescale is a highly desired trait for medical applications. Modifications are made to mERs using two different biopolymers, chitosan and alginate. Chitosan is adsorbed to the surface of mERs via charge interactions, and alginate is broken down and encapsulated inside the core of the mERs. Both provide a barrier to diffusion that slows the release of solutes loaded into mERs. The third application discussed is employing mERs as an MRI contrast agent. In a method similar to prior work with liposomes, lipids containing chelated gadolinium are incorporated into the mER membrane. Gadolinium is currently the most popular choice of element for contrast agents, and mERs provide unique qualities over other methods of delivery.

Chapter 2

Background

2.1 Vesicles and Liposomes

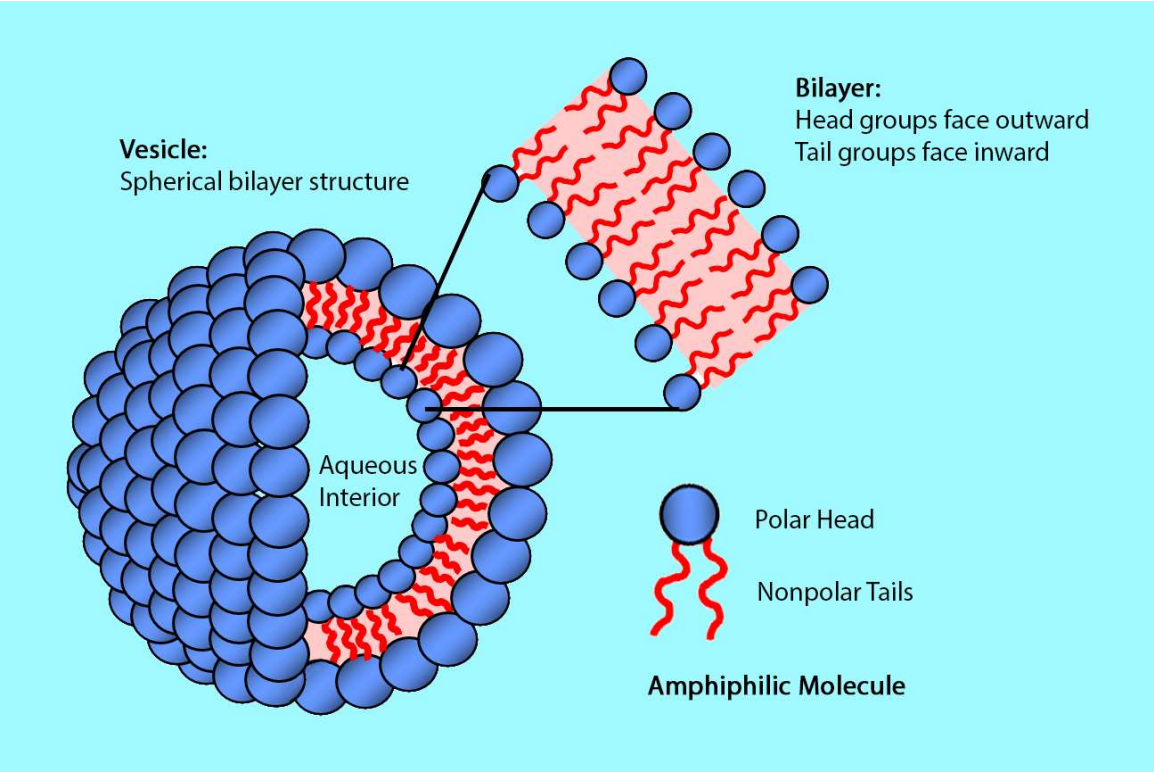

Figure 2.1. Diagram of Vesicle Structure[1]

Amphiphilic molecules have both hydrophilic (water-loving) and hydrophobic (water-fearing) parts. A typical example is the phospholipid, which has a polar head and two nonpolar tails and is a major constituent of cell membranes. Bilayers consist of two stacked sheets of amphiphilic molecules where the hydrophilic parts are oriented outward. This means the interior is hydrophobic while the exterior is hydrophilic. Vesicles, depicted in Figure 2.1., are spherical

enclosed bilayers. Vesicles-like structures have attracted considerable attention in bioengineering and medicine as micro to nano scale containers.

The most popular type of vesicle-like structure studied is the liposome. Liposomes are artificially constructed from a formulated mixture of lipids. They were first observed in the 1960s by Bangham et. al.,[2] and the term "liposome" was coined in the following decade.[3] Liposomes are assembled using methods of producing shear forces, including vigorous mixing, sonication, and extrusion. This is done in tandem with solubilization methods, including thin film hydration, injection/infusion, and reverse phase evaporation.[4,5]

In the literature, the liposome membrane has been modified with the addition of various molecules, including targeting antibodies, polyethylene glycol to extend circulation, stimuli-sensitive lipids, cell penetrating peptides, and viral components. Methods of administration include oral, topical, subcutaneous, inhalational, and intravenous. Applications include drug delivery, gene therapy, imaging agents, vaccines, and multi-functional devices.[6,7]

2.2 History and Properties of mERs

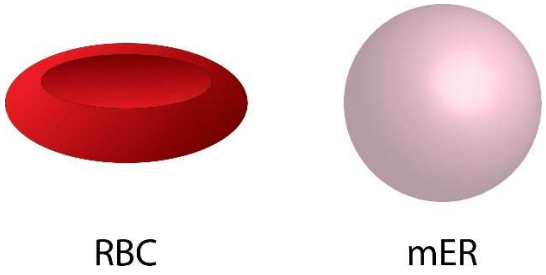

Figure 2.2. RBC and mER

Micro-erythrosomes (mERs), sometimes called "ghosts," are the result of removing the hemoglobin from the interior of red blood cells (RBCs) using an osmotic gradient. The name is a

portmanteau of erythrocyte (RBC) and liposome. mERs are essentially large vesicles, which are spherical membranes composed of amphiphilic molecules. An illustration of an RBC and an mER are depicted in Figure 2.2. The phenomenon of hemolysis (the rupture of erythrocyte membranes) was studied as early as the 1940s,[8] with early descriptions of erythrocyte ghosts arising around the 1960s.[9] mERs are typically compared to liposomes, which are smaller vesicles of artificial rather than natural origin. Due to the water-insoluble nature of the lipids, liposomes must be forcibly assembled using high shear.[5,10] Liposomes also have limitations regarding colloidal stability and biocompatibility.[11,12] The actual term "erythrosomes" appears to have been coined in a 1981 paper,[13] when describing a ghost-liposome hybrid. Interest in the subject waned for a while, only to be reinvigorated in recent years.

The size of mERs varies based on the source erythrocytes they are derived from.[14] The bovine mERs we work with are typically 3-4 microns in diameter. They have a negative surface charge (zeta potential around -30 mV), which helps prevent aggregation.[15] Whereas liposomes are generally thermodynamically unstable (tending to aggregate),[16] mERs can remain stable for months. mERs are able to circulate in vivo for longer periods of time than liposomes. Plain liposomes circulate for ~2 hours, and liposomes modified with polyethylene glycol (for steric stability) circulate for ~16-24 hours.[17] mERs, by contrast, can circulate for 3 or 4 days, as found in studies with dogs and rabbits respectively.[18,19] This higher circulation time is promising in that it increases the likelihood that mER drug carriers can reach their target before clearance by the immune system.

Related areas of study include nano-erythrosomes (nERs) and carrier erythrocytes. nERs are mERs that have been reduced in size using shear, yielding vesicles in the 100-200 nm range.[20,21] This allows them to be used in situations that require smaller containers, such as with inhalational delivery.[22] Carrier erythrocytes are RBCs that have been loaded with solute using only a single step of hypotonic hemolysis, meaning most of the hemoglobin is still present alongside the drug of choice.[23] They tend to be more robust than mERs, but cannot carry as much solute due to the space occupied by hemoglobin.[15,24,25]

2.3 Confocal Fluorescence Microscopy

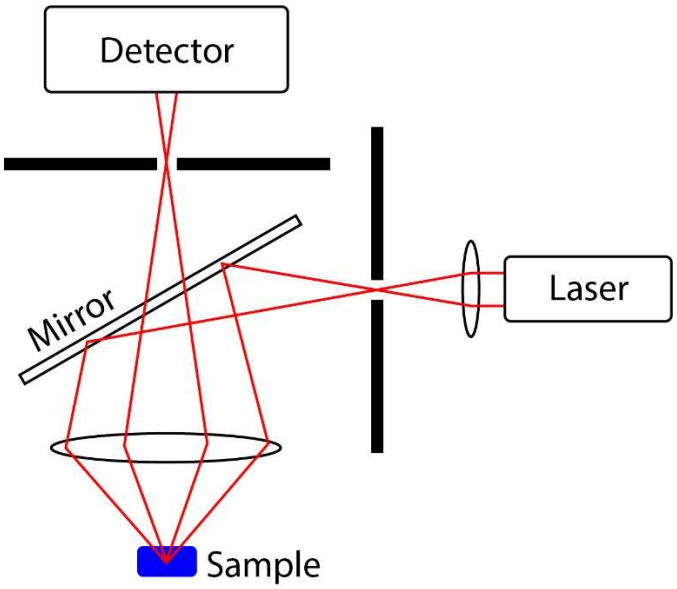

Figure 2.3. Confocal Microscopy

Traditional brightfield microscopy illuminates the entire sample evenly with light. Confocal microscopy works by using a point source of light, a beam splitter, and a pinhole to prevent all out-of-focus light from entering the detector. This increases the effective resolution of the image, while reducing blurring.[26] The drawback is a lower signal intensity, which means longer exposure times may be required. Essentially, each image taken with a confocal

microscope is a thin planar section of the sample (a hollow sphere would show as a ring rather than an opaque circle). The system is depicted in Figure 2.3.

For our images, we used a Zeiss LSM 710 Confocal Microscope. The device offers laser wavelengths at 405, 458, 488, 514, 561, and 633 nm. We primarily worked with red and green ranges, corresponding to DiI (a lipophilic cationic indocarbocyanine dye) and fluorescein respectively. We used a 40x oil-immersion objective for imaging.

2.4 Biopolymers

Biopolymers are chain macromolecules produced by living organisms. Their repeating units are typically carbohydrates, amino acids, or nucleic acids. Research interest in biopolymers is often due to their biocompatibility or their adaptability for modification. Hydrogels made of biopolymers have been investigated for their potential applications in drug delivery.[27] In this work, we make use of two specific biopolymers, chitosan and alginate.

Chitosan is a linear biopolymer consisting of D-glucosamine and N-acetyl-D-glucosamine units. It is primarily sourced from shrimp shells containing chitin, a polymer of fully acetylated glucosamine units. Treatment with a base (such as hydroxide) and further processing yields chitosan. Chitosan and its derivatives have seen use as biopesticides, filtration agents, preservatives, absorbents, and hemostatic agents.

Alginic acid, or alginate, is a linear biopolymer consisting of B-D-mannuronate and a-L-guluronate units. There are both homopolymeric blocks and blocks of alternating units. It is

primarily sourced from brown seaweed. A hot alkali solution (typically sodium carbonate) is used to extract the alginate from cell walls. It has been used as a thickening agent and as the base ingredient of hydrogels.

2.5 Release from Microstructures

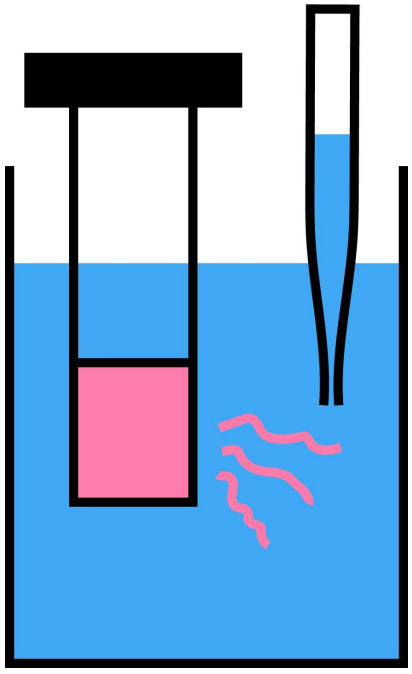

Figure 2.4. Schematic illustration of dialysis setup

To study the release of solutes from mERs, we load mERs with dye and place them in a dialysis setup, depicted in Figure 2.4. The mERs are placed in cellulose tubing, which is then placed in a larger reservoir of isotonic buffer with gentle agitation. The changing concentration of dye in the external solution is monitored using Ultraviolet-Visible (UV-Vis) spectroscopy. Non-bonding electrons on molecules can absorb ultraviolet or visible light, and the absorbance can be correlated with concentration.[28] The primary dye used is bromophenol blue, a negatively charged molecule with an absorbance peak at 590 nm. Prior to experiments, any molecule to be quantified with UV-Vis is first measured at prepared concentrations to create a standard curve. A

mass balance of the concentration inside and outside the dialysis tubing was used to verify the reliability of the method.

2.5 Contrast Agents

Magnetic resonance imaging (MRI) is commonly used in medicine for the diagnosis and staging of disease. A commonly used imaging agent is gadopentetic acid, which consists of a gadolinium ion (Gd3+) chelated by diethylenetriaminepentaacetic acid (DTPA).[29] DTPA has five carboxylic acid groups, three of which conjugate with Gd when chelating. Chelation is important because it prevents undesired side reactions that can occur with free metal ions.[30] Gadolinium is the element of choice for most contrast agents due to its paramagnetism, which shortens nuclear relaxation times. During MRI, the body tissues are exposed to a strong magnetic field, which polarizes hydrogen nuclei spins. A strong radio pulse is then applied to perturb the magnetization, and relaxation is the return to equilibrium. The detection of polarization is used to generate an image, and affecting the relaxation of protons in water molecules changes the contrast.

2.6 Cell Viability

It is desired to determine the cytotoxicity of an mER-based formulation. This requires the culturing of cells, incubation together with the mERs, and the measurement with a cell proliferation assay. We used the Premixed WST-1 Cell Proliferation Reagent. Its primary component is a tetrazolium salt, which is cleaved by mitochondrial enzymes (succinate-tetrazolium reductase) present in viable cells.[31] The product is formazan dye, a dark red molecule

with an absorbance peak at 440 nm. A multiwell plate reader is used to record absorbance values, from which the number of surviving cells can be calculated.

For microscopy, we use calcein AM, the acetomethoxy derivative of a fluorescent dye. Calcein AM is a non-fluorescent molecule, but esterases inside living cells can convert it into calcein, the anionic form which fluoresces with excitation and emission wavelengths of 495 and 515 nm respectively.[32] Thus, calcein AM allows the visualization of apoptosis, as staining will make living cells fluoresce bright green while dead cells will remain dark. It is particularly useful for monitoring damage due to the generation of reactive oxygen species.[33]

Chapter 3

mERs as Killer Cells

3.1 Introduction

The field of cancer medicine is always in need of new therapeutic techniques. Chemotherapy and radiation both have highly undesirable side effects, and surgery often cannot reliably remove the tumor. Tumors are typically hypoxic, i.e. they contain low levels of oxygen, and use oxygen-independent methods of generating ATP. This leads to a deficiency of antioxidative enzymes, making them more vulnerable to oxidative stress.[34,35] Thus, one strategy to kill tumor cells is to exploit that weakness by the employment of enzymes that generate reactive oxygen species (ROS). Studies have found that increased levels of hydrogen peroxide (H_2O_2), an ROS, can trigger programmed cell death (apoptosis) via the activation of caspase, an enzyme that regulates degradation of cellular components.[36-38] Accordingly, researchers have looked for ways to enzymatically generate ROS, including peroxide, in the vicinity of cancer cells. One such enzyme is glucose oxidase (GOx), which consumes glucose as a substrate. Cancer metabolizes external glucose for anaerobic fermentation as its primary energy source.[39] Therefore, GOx can both deprive tumors of an essential nutrient, as well as activate peroxide-dependent apoptosis. This dual action is a promising approach to cancer therapy.

Early investigation into the antitumor potential of GOx began in the 1980s, but the area has not attracted much interest until recently. This is because GOx alone has poor stability *in vivo*, is systemically toxic, and provokes an immune response. New studies in the past three years sought to deal with this by exploring different GOx delivery methods. Cheng et. al.

incubated GOx loaded biopolymer microbeads with cancer cells *in vitro*, but were only able to reduce cell viability by 30%.[40] Huo et. al., Li et. al., and Zhao et. al. reduced tumor growth in mice using GOx loaded into 260 nm porous silica nanoparticles, 110 nm polymersomes, and 800 nm nanogels respectively.[41-43] The three *in vivo* studies found no obvious systemic toxicity. There is also some related work showing virucidal[44] and fungicidal[45] applications, as well as studies on other ROS-generating enzymes such as amine oxidase.[46,47]

Although these past works have advanced the field, they have some major shortcomings. The nanogels and nanoparticles have an *in vivo* half-life of only a few hours. The microbeads are too large to use in the bloodstream, and the polymersomes are both expensive and difficult to prepare. To address all these issues, we propose a new method of delivery: encapsulation inside micro-erythrosomes (mERs). mERs are bilayer structures derived from the membranes of red blood cells (RBCs). mERs retain many of the characteristics of the parent RBCs, allowing them to circulate longer in vivo due to recognition by the immune system. They have a half-life of up to 7 days,[18] and are both simple and inexpensive to prepare.

To our knowledge, our work is the first example of using any kind of bilayer structure to deliver GOx for cancer-killing purposes, as well as one of the first studies on mERs for purposes beyond passive release. In our results, we will demonstrate the preparation of GOx mERs, measure their production of hydrogen peroxide, and examine their effect on SCCHN (Squamous Cell Carcinoma of the Head and Neck) 15B cells, a human cancer line. We report a drop in cell viability of over 90% for a small concentration of GOx mERs.

3.2 Experimental Section

Materials. Glucose oxidase, WST-1 Cell Proliferation Reagent, and phosphate buffered saline (PBS) were obtained from Sigma Aldrich. Hydrogen peroxide was obtained from EMD Millipore. 15B cells and cell culture medium were provided by Dr. William Bentley's laboratory. Adult bovine blood was obtained from Lampire Biological Laboratories.

Preparation of mERs. Whole blood was centrifuged at 3000 rpm for 5 min at 4 °C and the supernatant was removed. The sediment was diluted in 1x PBS, and centrifuged for 3 more cycles, removing the supernatant and the buffy coat. Resulting RBCs were diluted in 0.1x PBS. The suspension was centrifuged at 12000 rpm for 15 min at 4 °C and the supernatant is removed. Dilution in fresh 0.1x PBS and centrifugation continued until mERs were a pale off-white color.

Fluorescent mERs. 1 μM of DiI was dissolved in ethanol. 0.2 mL of the DiI was mixed with 0.4 mL mERs. 1.4 mL of 10x PBS was added and the mixture was centrifuged at 10000 rpm for 12 min at 4 °C. The supernatant was removed, and the mERs were washed twice with 1x PBS.

Encapsulation of Solutes in mERs. mERs were incubated for 30 min at 4 °C in 0.1x PBS containing dissolved solute of interest. The mixture was centrifuged and resuspended in 10x PBS. The solution was warmed at 37 °C for 30 min and then centrifuged, resuspending in 1x PBS.

Preparation and Testing of GOx mERs. mERs were loaded using a stock solution of 232 U/mL GOx, using the normal encapsulation method. 1 U of GOx mERs was set as 1 part

centrifuged (high-density) mERs and 3 parts PBS. 1 mL of 1 U GOx mERs were placed in dialysis tubing in a reservoir of 0.2 M glucose. Samples were taken (in triplicate) from the reservoir and peroxide concentration was measured by UV-Vis at 240 nm absorbance.

Killer Cell Experiment. 15B cells were cultured and transferred to a 96-well plate. 6 rows were used: 2 each at 15k, 30k, and 50k cells. 10 columns were used: 1 for media only, 1 for cells only, 1 for cells and normal mERs, and 7 for GOx mERs. Each well was prepared with 200 μL cell culture media and 60 μL of mERs. An outer ring of buffer was used to mitigate evaporation. Cells were incubated for 22 hr. Cell proliferation reagent WST-1 was added in a 1:10 ratio (typically 26 μL for a well with 260 μL total volume). The plate was incubated for 30 min and then shaken for 1 min. Absorbances were read at 440 nm with a multiwell plate reader.

Dynamic Study. 15B cells were cultured and transferred to a 96-well plate. 5 rows of 50k cells were used along with one row of media, with an outer ring of buffer. 60 μL of GOx mERs were added at 3 hr time intervals. Some wells were reserved for controls and background. At the end of 24 hr, WST-1 was added in a 1:10 ratio. The plate was incubated for 30 min and then shaken for 1 min. Absorbances were read at 440 nm with a multiwell plate reader.

Preparation of cells for imaging. DiI-tagged mERs were incubated with 15B cells. 200 μL samples were taken from wells and centrifuged at 1500 rpm for 30 s. The sediment contains 15B cells; the supernatant containing mERs is removed and centrifuged at 10000 rpm for 15 min. A 1x standard working solution of Calcein AM is diluted by a factor of 1000 in 1x PBS. 100 μL of dilute Calcein AM is added to the 15B cells, mixed gently, and allowed to react for 5 min. The

resuspended cells were then centrifuged again at 1500 rpm for 30 sec. The supernatant is discarded, and the cells and mERs were recombined together with 10 µL of 1x PBS. The final solution is gently mixed and 10 µL is withdrawn for microscopy.

3.3 Results and Discussion

Preparation and Characterization of Micro-Erythrosomes (mERs)

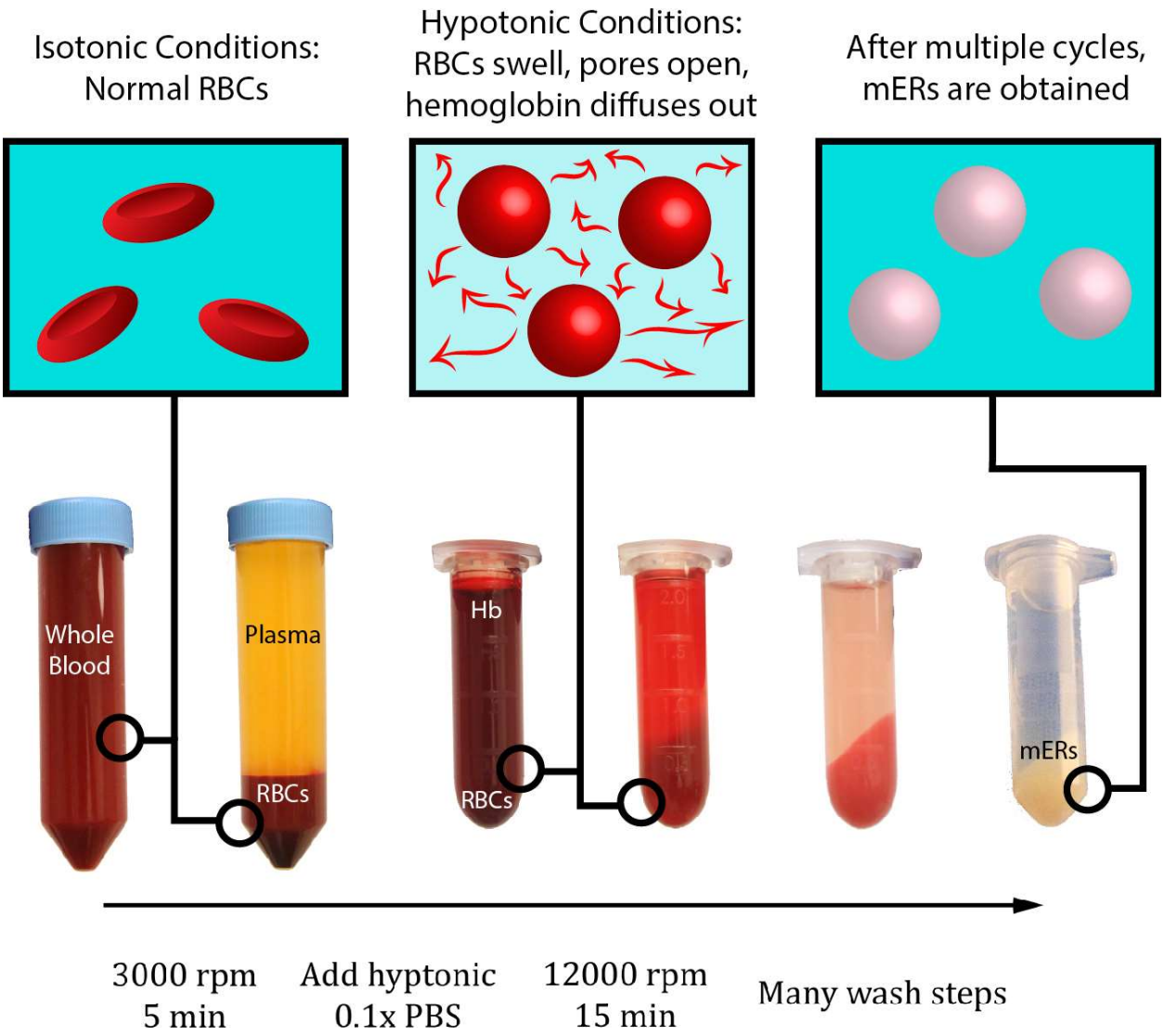

Figure 3.1. Schematic of mER Preparation Process. RBCs are isolated, and diluted in hypotonic PBS to release hemoglobin. mERs are obtained by multiple centrifugation steps

The process for preparing mERs is depicted in Figure 3.1. This is a simple hypotonic dilution method. The starting material is adult bovine blood, which consists of about 20% RBCs. With a cytometer, this was measured to be roughly 3 x 10^9 RBCs per mL of blood. The density difference between RBCs and other components of the blood allows for separation by centrifugation. After removing the first supernatant containing mostly plasma and platelets, RBCs are washed twice with an isotonic (equal osmotic pressure inside and outside the cell) buffer. Residual plasma in the supernatant is removed, as well as the thin coating of white blood cells.

Isolated RBCs are then diluted in hypotonic (osmotic pressure inside the cell is greater than outside) buffer, which causes the cells to swell with water and pores to open in the membrane.[48] Pore formation is associated with the clustering of band 3 membrane proteins[49-52] the rearrangement of phospholipids,[53,54] and a change in membrane viscoelasticity typically mediated by the cytoskeletal protein spectrin.[55,56] Hemoglobin is then able to leak out into solution. The swollen cells, having also lost some of their contents, are now less dense, thus requiring a larger force to separate. They are centrifuged several times at higher speeds, removing the hemoglobin-rich supernatant each time. The final result is a sediment of pale, off-white (sometimes tinted pink or yellow) mERs. These are resuspended in isotonic buffer.

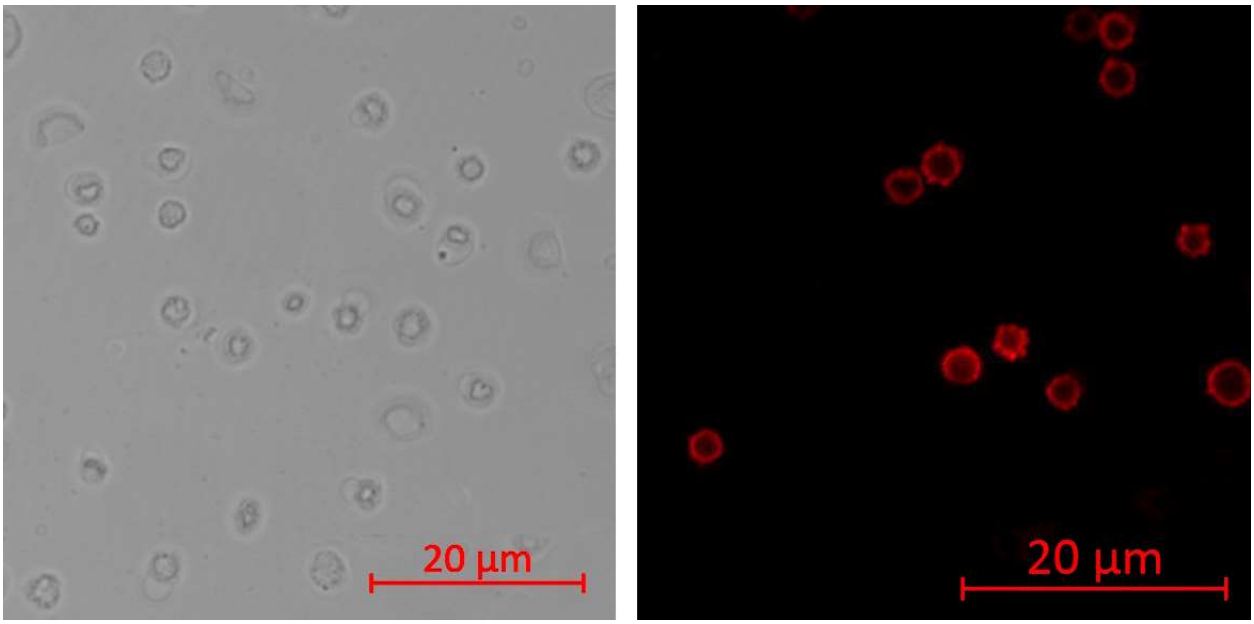

Figure 3.2. Microscope Images of mERs. Transmitted light on the left and fluorescence on the right, both taken with a confocal microscope

Transmitted light and fluorescence microscopy images of mERs are shown in Figure 3.2. To obtain fluorescent mERs, they are tagged with a lipophilic cationic carbocyanine dye called DiI. DiI is dissolved in ethanol and then mixed with mERs. The ethanol solubilizes the DiI and interrupts the membrane, allowing DiI to be incorporated. The mERs are centrifuged, and then resuspended in hypertonic buffer. They are washed a few times with isotonic buffer to yield fluorescent mERs. Due to their high transparency, transmitted light provides better contrast than traditional brightfield microscopy. Together with fluorescence, we can see the size and structure of mERs. They are spherical with a diameter of 3.1 ± 0.3 µm.

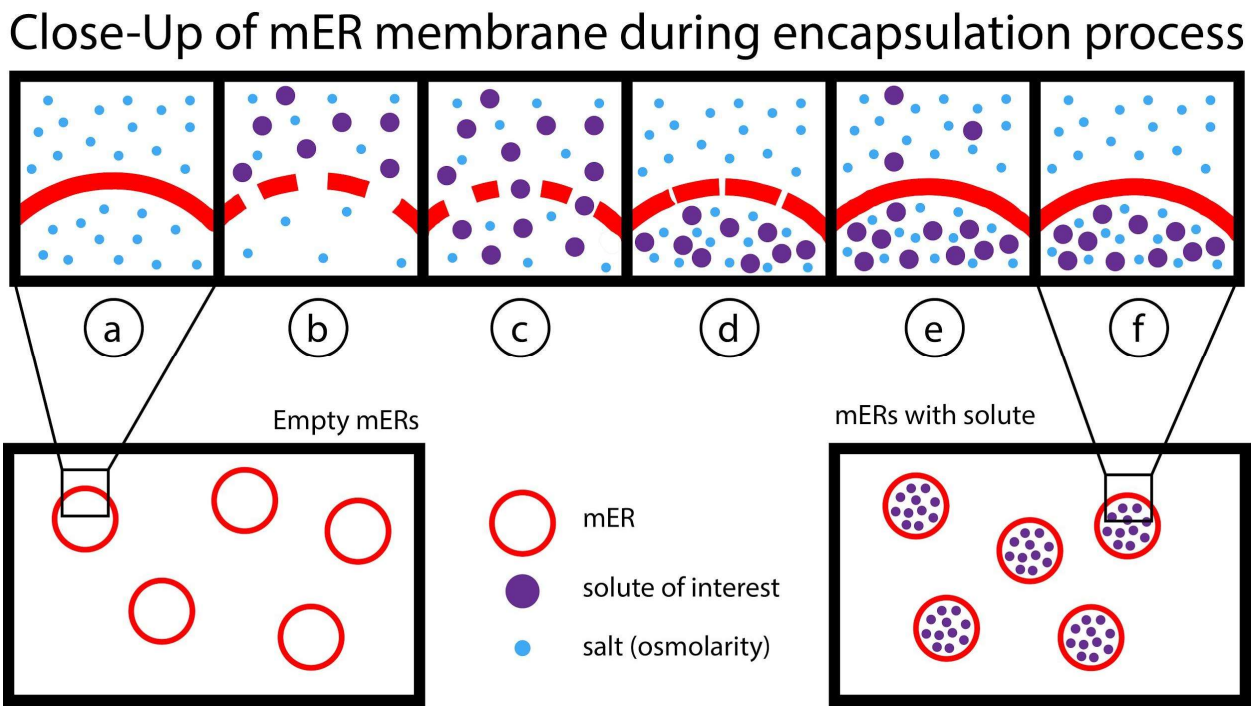

Figure 3.3. Solute Encapsulation Process. (a) mER in isotonic buffer (b) mER in hypotonic buffer with solute (c) solute enters mER (d) mER transferred to hypertonic buffer (e) solution warmed to 40 C to reseal (f) washed with isotonic buffer

The process for encapsulating cargo in mERs is shown in Figure 3.3. First, mERs are diluted in hypotonic buffer containing the dissolved solute of interest. As during the preparation process, the mERs swell and pores open up allowing the solute to enter. After enough time for the concentration across the membrane to reach equilibrium, the mERs are isolated by centrifugation and resuspended in hypertonic buffer. This suspension is then heated to 37 °C, which provides energy for the membrane to "reseal" itself.[57] This is an accepted process in the literature,[58,59] used to reduce the loss of solute during preparation. It has been hypothesized that resealing occurs by rearrangement of membrane lipids, returning to a low-energy equilibrium configuration.[60] The mERs are then washed with isotonic buffer to remove any free solute. The final result is mERs loaded with a desired cargo.

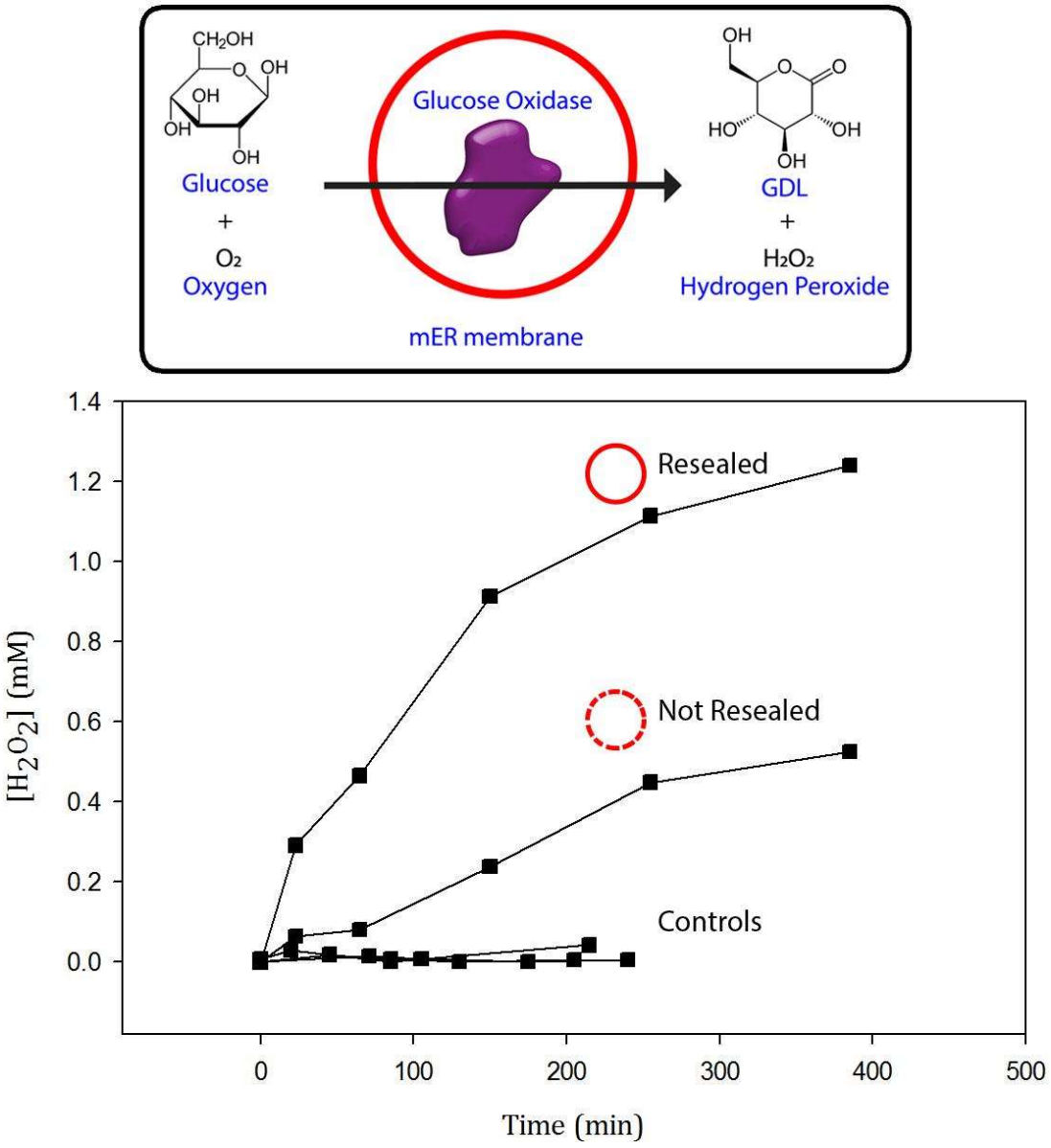

Figure 3.4. Peroxide Production by GOx mERs

Glucose oxidase (GOx) is an enzyme that catalyzes a reaction depicted in Figure 3.4. GOx is loaded into mERs using the standard encapsulation process discussed previously. We measured the production of hydrogen peroxide by GOx mERs using UV-Vis. Three controls were used: one trial with normal mERs containing no GOx, one trial with no glucose in the reservoir, and one trial using the supernatant from a GOx mER suspension (to show that there is no leakage of GOx after preparation). Additionally, one trial was conducted using GOx mERs

that had not been resealed (no heating conducted after encapsulation). As expected, the resealed GOx mERs retained more GOx, leading to higher production of peroxide.

Killing Cancer Cells with GOx mERs

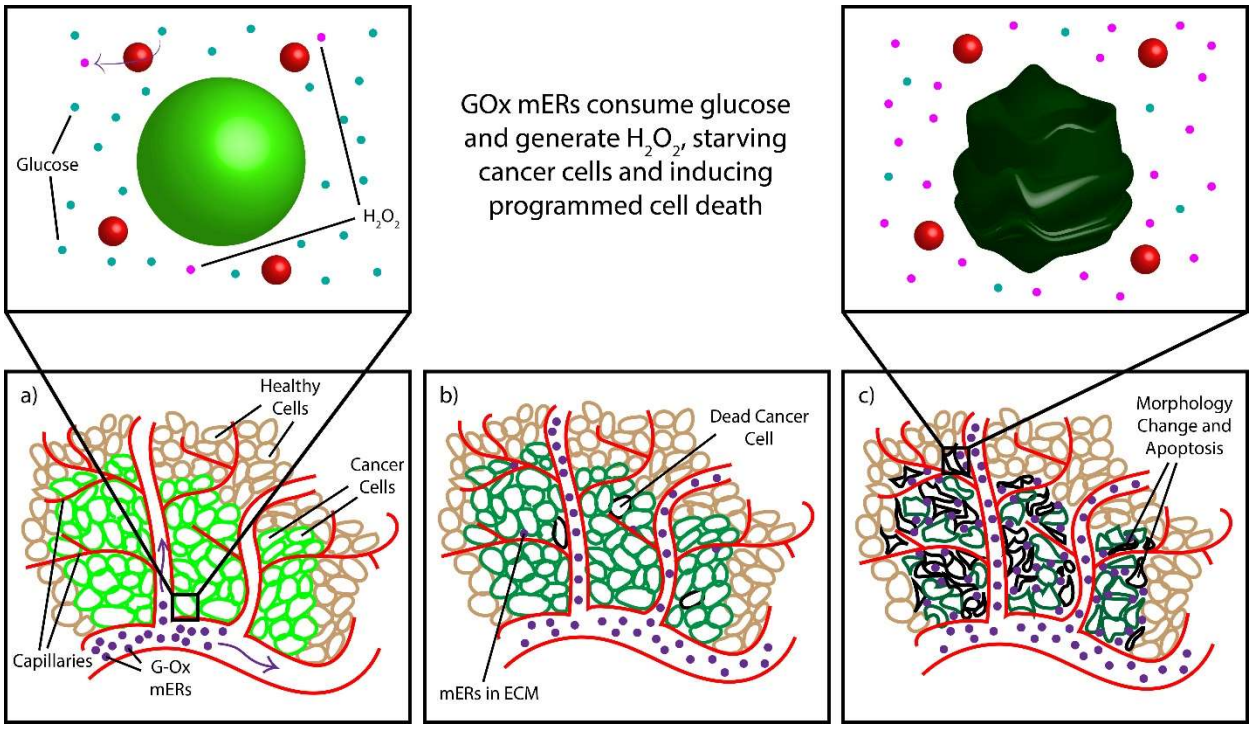

Figure 3.5. mERs as Killer Cells. (a) mERs enter the tumor via the bloodstream (b) mERs consume glucose and generate peroxide (c) the tumor is extensively damaged

Glucose is present both *in vitro* (as a component of cell culture media) and *in vivo* (dissolved in the blood), providing the necessary fuel for generating peroxide. As peroxide concentrations rise, cells undergo apoptosis (cell death), which is often accompanied by a change in morphology. A schematic of mERs killing cancer cells in the body is shown in Figure 3.5. To lay the groundwork for this future application, we will study the killing of cancer cells *in vitro*.

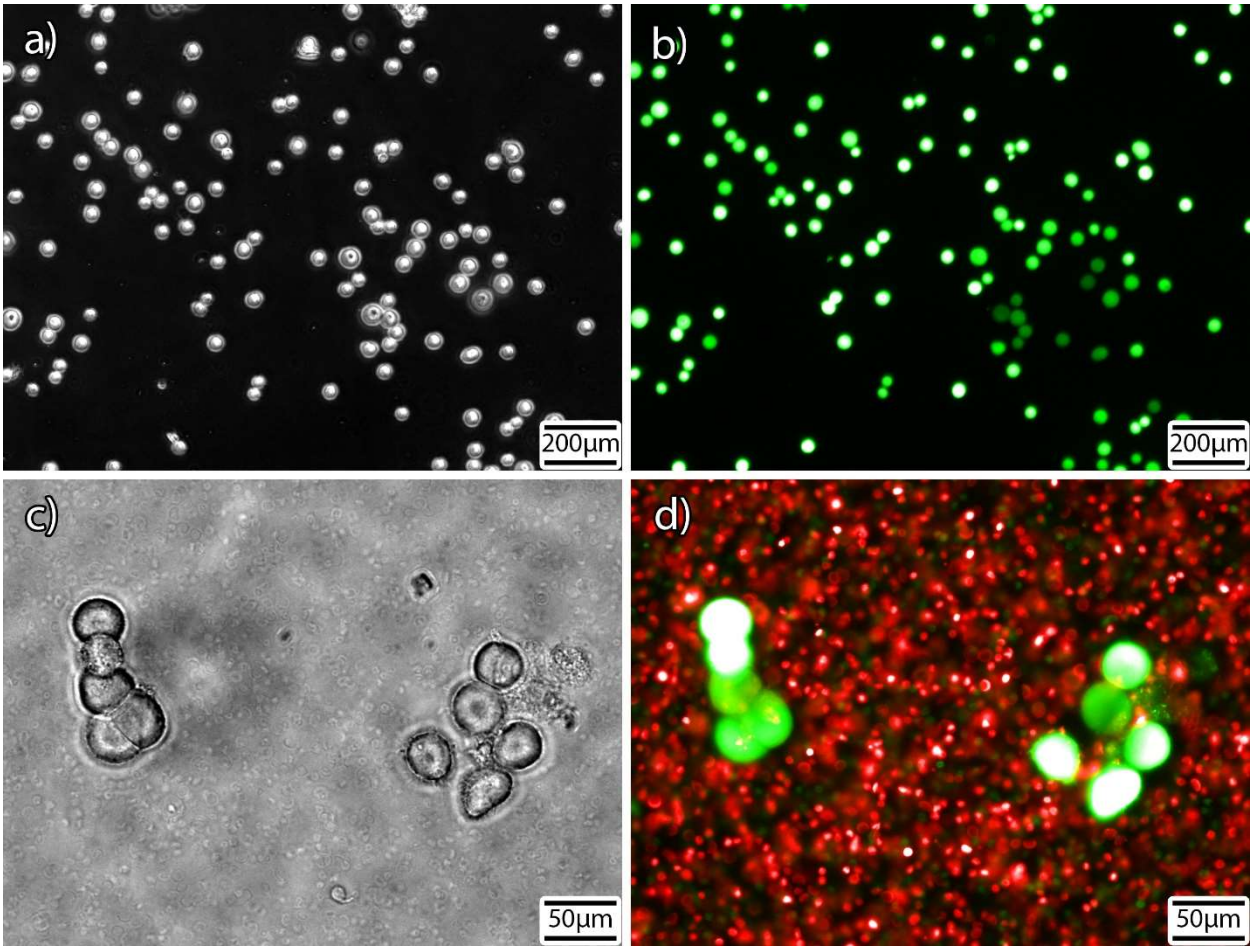

Figure 3.6. Microscopy of Control Samples. (a) brightfield image of healthy 15B cells (b) fluorescence image of healthy cells (c) brightfield image of cells with empty mERs (d) fluorescence image of cells with empty mERs

For controls, we examine two cases: the first consists of 15B cells without the presence of mERs; the second consists of 15B cells incubated with mERs that do not contain GOx. The cells are stained with Calcein AM, which interacts with products of the cell's metabolism. Healthy cells will fluoresce a bright green, whereas unhealthy or dead cells show up as dark green or not at all. Both of our controls have been incubated for 6 hours, and are shown in Figure 3.6. As expected, neither sample indicates any deterioration in cell health. The cells fluoresce brightly, show normal adherence to each other in some areas, and display no changes in morphology.

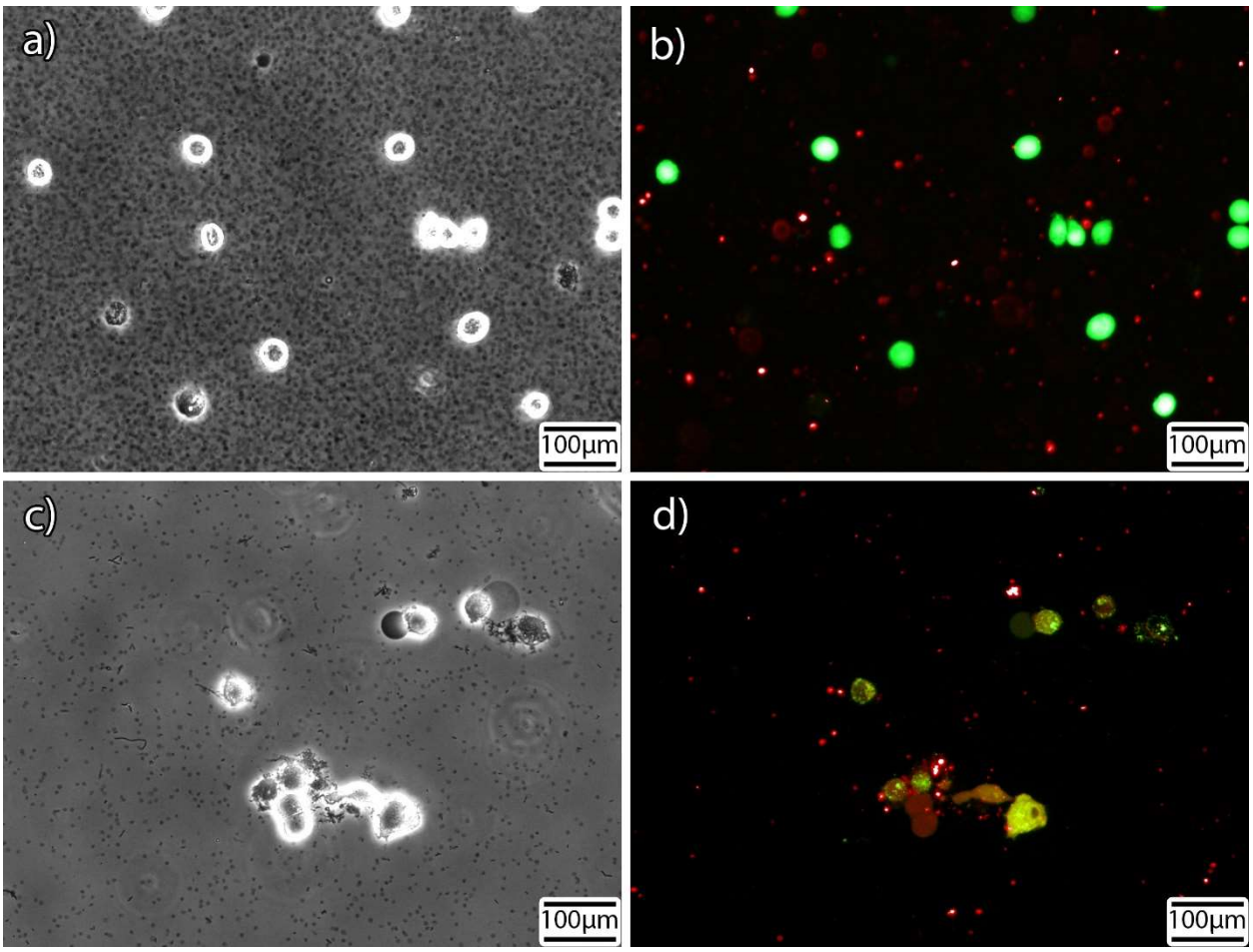

Figure 3.7. Microscopy of Killer Cells. (a) brightfield cells incubated with GOx mERs for 6 hr (b) fluorescence of cells incubated with GOx mERs for 6 hr (c) brightfield cells incubated with GOx mERs for 24 hr (d) fluorescence of cells incubated with GOx mERs for 24 hr

Samples of cells incubated with GOx mERs for 6 hr (above) and 24 hr (below) are shown in Figure 3.7. In the 6 hr sample, several cells that appear in the field of view of the brightfield image are dark in the fluorescence image. This indicates that they are dead, which is further corroborated by some minor changes in morphology. The geometries of some cells have become less spherical, and in some cases protrusions on the surface can be observed. In the 24 hr sample, many more of the cells have died. Changes in morphology are more drastic, and small fragments of cells can be seen. Some cells have become stretched, and others appear to have burst or been

torn apart. The few surviving cells fluoresce only weakly, indicating that they are also undergoing apoptosis.

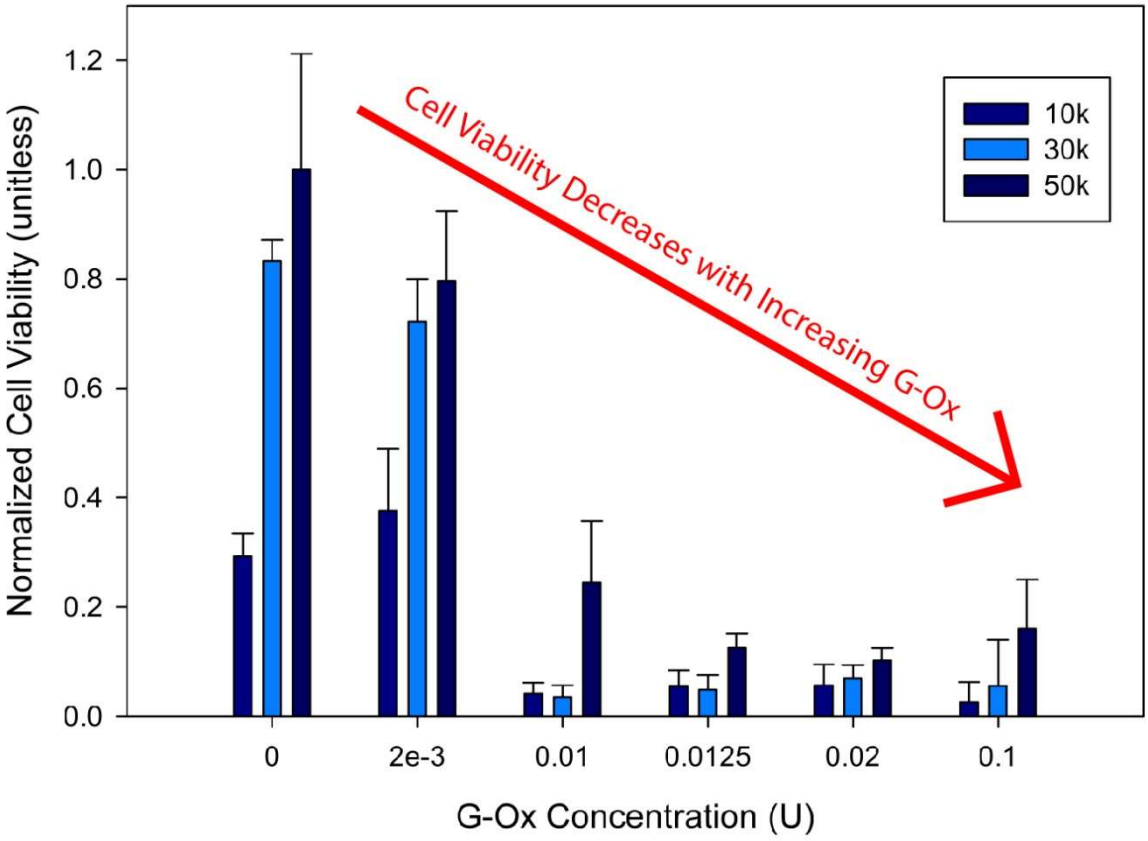

Figure 3.8. Overnight incubation of GOx mERs

The results of absorbance readings from 22 hr incubation of cells with GOx mERs are shown in Figure 3.8. A reagent that reacts with metabolic products to form a red dye is used to measure cell viability, which is then normalized to the control case on the far left. Various concentrations of GOx mERs were tested, along with different initial densities of cells (10k, 30k, and 50k per well). Each point is an average of two wells. All values are normalized with respect to the largest value, corresponding to the 50k control. As expected, a higher cell seeding

concentration resulted in higher cell viability, and a higher concentration of GOx mERs resulted in lower cell viability. The threshold for a high degree of cell destruction appears to be around 0.01 U of GOx mERs. At those concentrations, for nearly all cases, cell viability is reduced by over 80%.

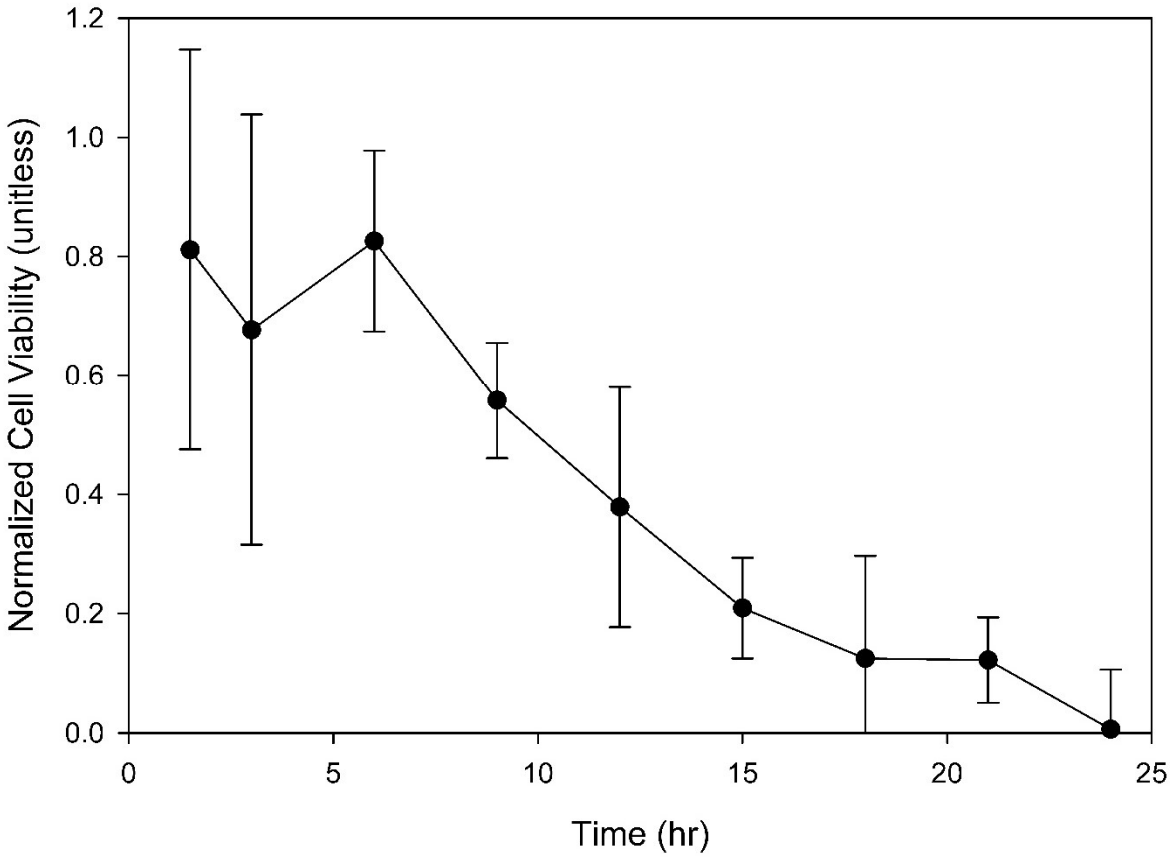

Figure 3.9. Kinetics of GOx mERs

The results of cells incubated with 0.01 U of GOx mERs for 24 hr are shown in Figure 3.9. Cell viability was measured in the same manner as before, averaging two wells per point. All values are normalized to a control, which is not shown. As expected, cell viability decreases over time, reaching a point where over 90% of the cells are killed.

3.4 Conclusions

In this study, we isolated erythrocytes from bovine blood and transformed them into micro-erythrosomes (mERs). The mERs were then loaded with glucose oxidase (GOx), and their ability to produce hydrogen peroxide in glucose solution was quantified. The GOx mERs were then evaluated for their ability to kill human cancer cells *in vitro*. GOx mERs at concentrations greater than 0.01 U are found to kill up to 90% of cancer cells compared to controls after 24 hour incubation. This killing action is corroborated by both qualitative (microscopy) and quantitative (absorbance) data.

These results demonstrate the viability of GOx mERs for the killing of cancer cells, and in the flexibility of mERs in general when it comes to accomplishing specialized tasks. Together with the existing advantages of mERs, we believe that further improvements to technique and additional functionalization can give mERs a wide array of novel applications in bioengineering and medicine.

Chapter 4

Enhancing the Capabilities of mERs

4.1 Introduction

Drug delivery is a major aspect of medical research with much room for improvement. Work in this field mainly focuses on designing containers for the drugs and improving their performance. Controlling the rate of release from those containers can ensure that more of the drug reaches its target, which both increases the effectiveness of treatment and decreases possible damage to healthy tissue. Two of the studies in this chapter aim to prolong the time scale of release from mERs.

In the first study, we adsorb chitosan to the surface of mERs. This layer of chitosan presents an additional barrier to diffusion, slowing down release of solutes from mERs. In the second study, we decrease the molecular weight of alginate using peroxide[61] so that it can be encapsulated inside mERs. The alginate is still large enough that it doesn't leak out under isotonic conditions (much like hemoglobin or other proteins), and it slows diffusion from mERs due to increased internal viscosity. Fluorescent chitosan and alginate are synthesized to visualize the two systems.

Another important facet of medical research is the diagnosis of disease. Magnetic resonance imaging (MRI) is used extensively to locate and determine the progression of disease. Sometimes, a contrast agent is administered to the patient to enhance the clarity of images taken by MRI. In the third study of this chapter, we seek to design a contrast agent based on mERs.

Prior work has been done where lipids containing chelated gadolinium were incorporated into liposomes. There has also been related work where lipoproteins were labeled with chelated indium.[62] Compared to liposomes, mERs are have a longer circulation time, have room for more surface modification, and can carry larger quantities of other cargo. This makes them better candidates to serve as multi-functional devices.

4.2 Experimental Section

Materials. Chitosan, alginate, carboxyfluorescein, aminofluorescein, 1-ethyl-3-(3-dimethylaminopropyl)carbodiimide (EDC), N-hydroxysuccinimide (NHS), octadecylamine (stearylamine), diethylenetriaminepentaacetic dianhydride (DTPA-dianhydride), gadolinium chloride, and phosphate buffered saline (PBS) were obtained from Sigma Aldrich. Methanol and ethanol were obtained from Pharmco-Aaper. Hydrogen peroxide and ammonium chloride were obtained from EMD Millipore. Ammonium hydroxide was obtained from J.T. Baker. Chloroform was obtained from TCI America. Hydrochloric acid was obtained from BDH chemicals. Dimethylformamide was obtained from Acros Organics. Adult bovine blood was obtained from Lampire Biological Laboratories.

Fluorescent Chitosan. 0.1 g of chitosan was dissolved in 10 mL of 0.2 M acetic acid. 0.024 g of carboxyfluorescein was dissolved in 400 mL of DI water. 0.011 g of NHS and 0.015 g of EDC were dissolved in 1 mL of DI water. The three solutions were mixed and the container was covered with aluminum foil. The mixture was stirred at 60 °C for 6 hr and allowed to sit at room temperature overnight. Sodium hydroxide was added to precipitate the chitosan, which was recovered by vacuum filtration. The product was returned to neutral pH, washed, and dried.

Preparation of Chitosan mERs. 500 µL of 1 wt% chitosan solution was mixed with 500 µL of mERs. The mixture was centrifuged at 10000 rpm for 10 min and washed three times. The chitosan mERs were incubated overnight with a saturated solution of bromophenol blue. The loaded mERs were washed once and then release was measured using dialysis.

Fluorescent Alginate. 0.1 g of alginate was dissolved in 10 mL of DI water. 0.5 mL of 30% hydrogen peroxide was added. The solution was heated and stirred at 50 °C for 2 hr. 0.02 g of aminofluorescein was dissolved in 10 mL of methanol. 0.01 g of NHS and 0.014 g of EDC were dissolved in 10 mL of DI water. The solutions were heated to 60 °C and mixed, diluting with water to a total volume of 120 mL. The mixture was stirred at 60 °C for 6 hr and allowed to sit at room temperature overnight. Hydrochloric acid was added to precipitate the aminofluorescein, and centrifugation was used to separate it. The product was washed with methanol and water. The pH was then adjusted to neutral, and the remaining product was dried.

Preparation of Alginate mERs. 1 mL of 30% hydrogen peroxide was added to 19 mL of 2 wt% alginate solution. The mixture was stirred at 50 °C for 2 hours to degrade the alginate. The resulting low-MW alginate was washed and dried. Low-MW alginate was loaded in mERs using the standard encapsulation process. The alginate mERs were incubated overnight with a saturated solution of bromophenol blue. The loaded mERs were washed once and then release was measured using dialysis.

Preparation of DTPA-BSA. This procedure is adapted from Jasanada et. al.[16] 0.539 g of stearylamine was dissolved in 40 mL of chloroform. 0.393 g of DTPA-dianhydride was dissolved in 50 mL of dry dimethylformamide. The DTPA solution was heated to 40 °C with stirring and stearylamine was added gradually over 1 hr. The mixture was allowed to react for another hour, and then allowed to cool. The precipitated product was separated with vacuum filtration, washed with acetone, and dried. The product was then recrystallized in boiling ethanol, washed with water, and dried.

Integration of DTPA-BSA. 7 g of ammonium chloride is dissolved in 60 mL of 30% ammonium hydroxide. The pH of the buffer was adjusted to 9.5. A less concentrated buffer was obtained by diluting the solution by a factor of 10. 0.05 g DTPA-BSA was dissolved in 20 mL of dilute buffer to yield a 2.8 mM solution. 200 µL of DTPA-BSA solution is mixed with 200 µL ethanol and 400 µL mERs. 400 µL of 10x PBS is added and the mixture is centrifuged at 3000 rp for 5 min. The supernatant is removed and centrifuged at 10000 rpm for 15 min. Gadolinium citrate is prepared by the addition of 2 mL of 17.5 µmol gadolinium chloride in HCl (pH 1) to 8 mL of 87.5 µmol aqueous sodium citrate. The modified mERs are washed with 1x PBS and then 400 µL of Gd citrate is introduced. The contrast agent mERs are washed again with 1x PBS.

4.3 Results and Discussion

Chitosan Coated mERs

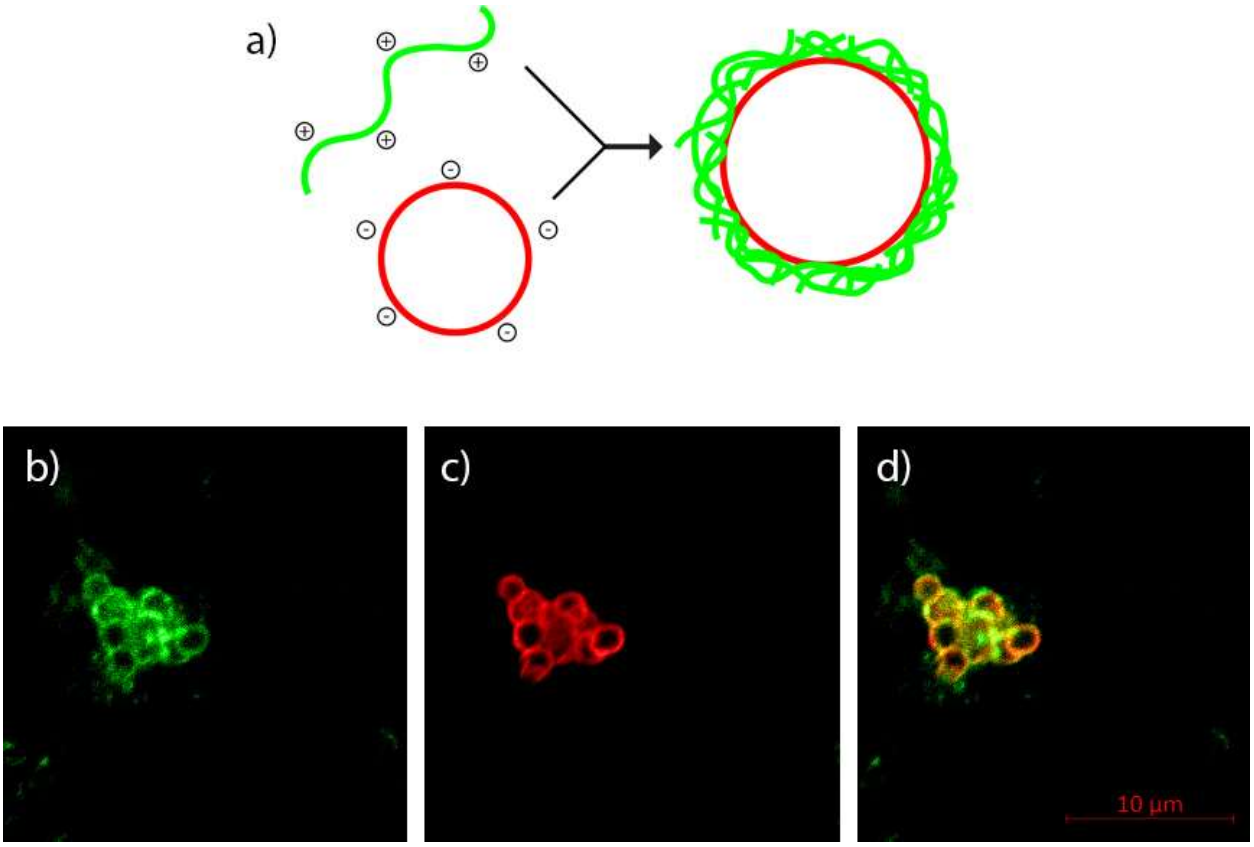

Figure 4.1. Chitosan Coated mERs. (a) Schematic Illustration (b) Green Fluorescence (c) Red Fluorescence (d) Combined Channels Image

The adsorption of chitosan onto the surface of mERs is depicted in Figure 4.1, where mERs are tagged with red DiI and chitosan has been modified with green fluorescein groups. We mix a 1 wt% chitosan solution with mERs, and then wash away the free chitosan. Some chitosan remains adsorbed to the surface due to charge interactions. The resulting chitosan-coated mERs appear to cluster to some extent. This aggregation may be due to the overall charge of the mERs becoming more neutral.

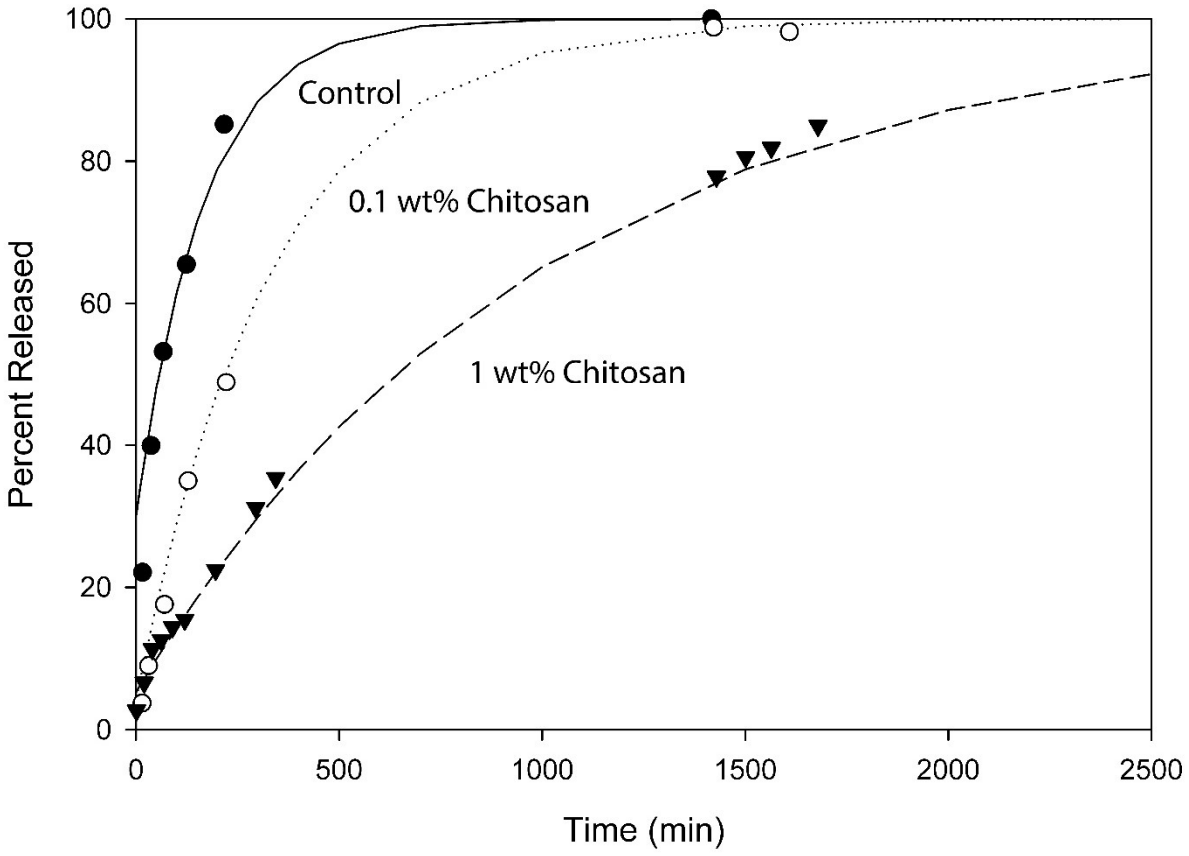

Figure 4.2. Release from Chitosan Coated mERs

The release of bromophenol blue dye from chitosan coated mERs is shown in Figure 4.2. The control is normal mERs without chitosan. Two different concentrations of chitosan are used during the adsorption process, with the higher concentration resulting in slower release. The control released 50% of the dye at ~57 minutes, while the 1 wt% chitosan released 50% at ~640 minutes. These results show that chitosan can slow down the diffusion of solutes from mERs.

Alginate Core mERs

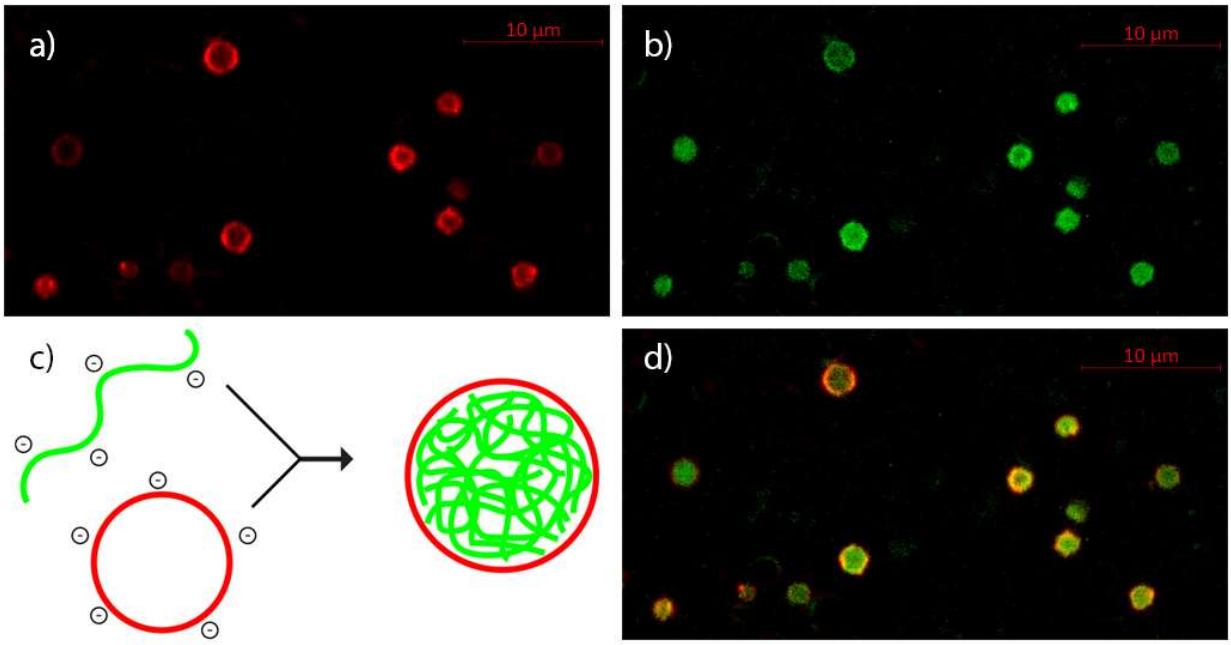

Figure 4.3. Encapsulation of Alginate in mERs. (a) Red Fluorescence (b) Green Fluorescence (c) Schematic Illustration (d) Combined Channels Image

The encapsulation of alginate inside mERs is depicted in Figure 4.2, where mERs are tagged with red DiI and alginate has been modified with green fluorescein groups. We first degrade alginate from a molecular weight (MW) of ~120 kDa into smaller fragments using hydrogen peroxide and heat. The small-MW alginate is then loaded into mERs using the standard encapsulation procedure discussed in the previous chapter. Microscopy shows that the alginate fills the interior of the mER and is fully enclosed. There is no apparent aggregation or damage to the alginate-core mERs.

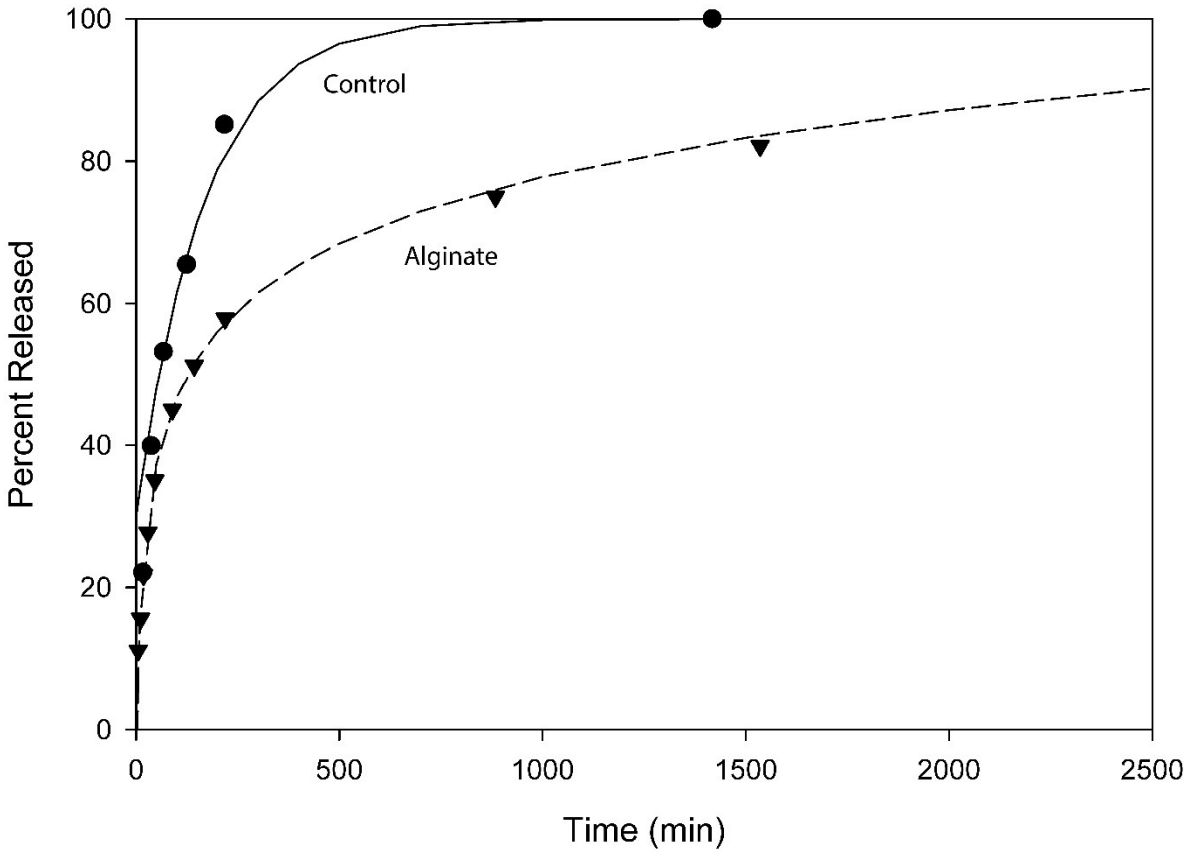

Figure 4.4. Release from Alginate Core mERs

The release of bromophenol blue dye from alginate core mERs is shown in Figure 4.4. The control is normal mERs without alginate. Alginate appears to slow the release, but in a manner that changes the behavior of the release curve. This may be due to an increase in internal viscosity. By the Einstein relation, an increase in viscosity increases diffusion constant. The control released 50% of the dye at ~57 minutes, while the alginate mERs released 50% of the dye at ~129 minutes. These results show that alginate can slow the diffusion of solutes from mERs.

Contrast Agent mERs

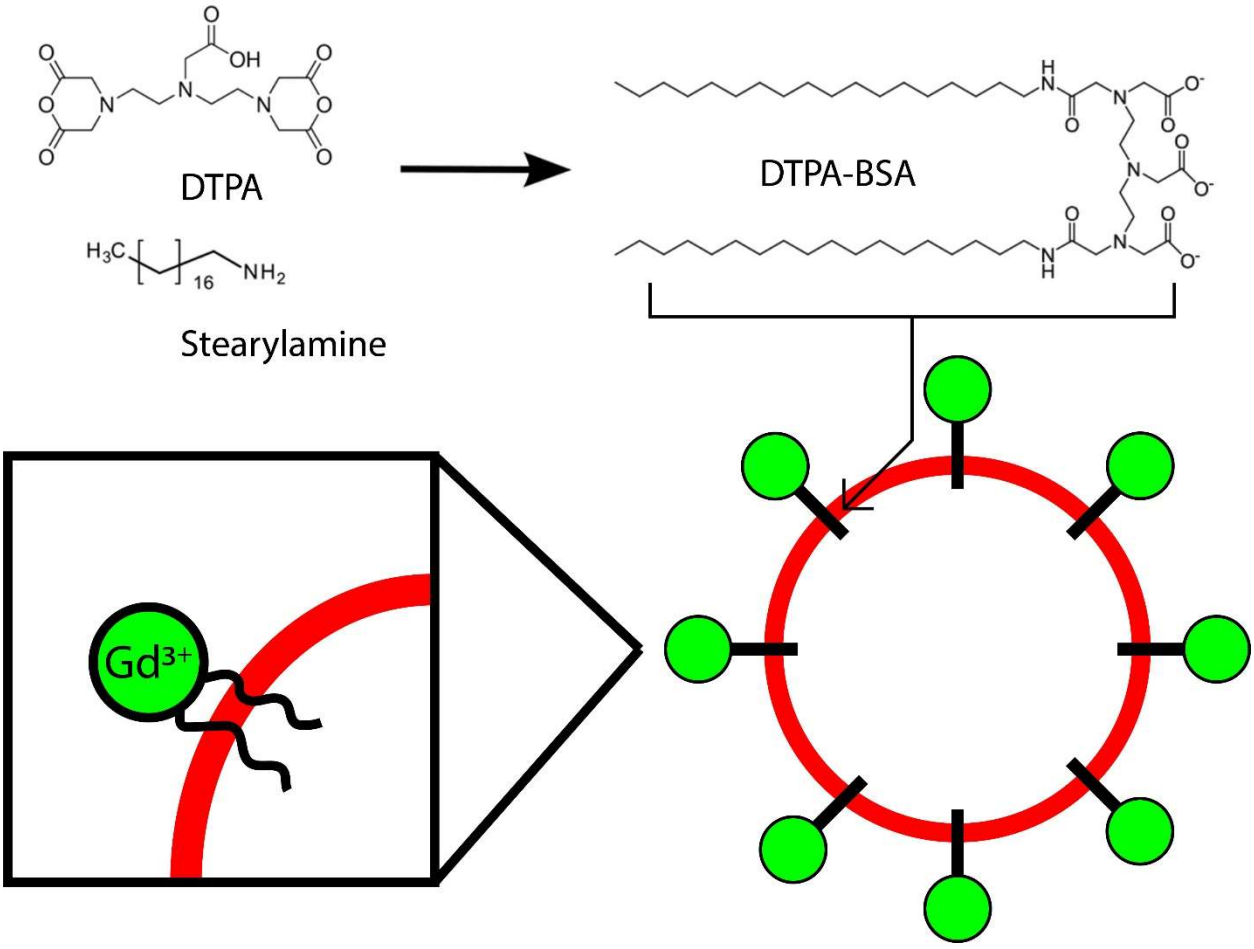

Figure 4.5. Schematic of mERs as a Contrast Agent

The preparation of an mER contrast agent is depicted in Figure 4.5. First, we must synthesize a chelator lipid that consists of DTPA linked with two stearylamine units, or DTPA-bistearylamide (DTPA-BSA). This lipid can be integrated into the mER membrane, and from there citrate can be used as a transfer agent for Gd. Citrate, like DTPA, is a chelator, but it has a weaker affinity. Thus, Gd will transfer from the citrate to the DTPA-BSA when the two come into contact. The reason for this additional step (as opposed to directly integrating Gd-DTPA-BSA into mERs), is that Gd-DTPA-BSA is only soluble in a chloroform-methanol mixture.

Chloroform is highly damaging to mERs, so it cannot be used. However, DTPA-BSA without Gd is soluble in ammonia buffer, which allows the mERs to be kept intact during the process.

Figure 4.6. Verification of DTPA-BSA. Left vial contains DTPA-BSA and Gd Citrate, right vial contains Gd Citrate and DI Water

Confirmation of the successful synthesis of DTPA-BSA is shown in Figure 3.6. The completed lipid is colorless when dissolved in ammonia buffer. Unreacted stearylamine would produce a turbid solution. When mixed with gadolinium citrate, DTPA-BSA becomes turbid due to insolubility. Unreacted DTPA would remain colorless while chelating gadolinium. Therefore, the final product must be DTPA-BSA. Dissolved DTPA-BSA is mixed with ethanol and mERs. The ethanol interrupts the membrane to allow for incorporation of the lipid, much like the process used to prepare fluorescent mERs. After wash steps, gadolinium citrate is added. After more wash steps, contrast agent mERs are obtained.

4.4 Conclusions

In the first two studies, mERs were modified to have chitosan adsorbed on the surface and alginate encapsulated inside. The resulting chitosan coated and alginate core mERs were imaged, and their rates of releasing solute were measured. Compared to normal mERs, the chitosan and alginate yielded release that was roughly 10 times and 2 times slower, respectively. The chitosan mERs tend to cluster, which is a phenomenon that needs to be addressed in the future if they are to be used for drug delivery applications. Overall, these results demonstrate promising ways to extend release from mERs. In the third study, a chelator lipid DTPA-BSA was synthesized. This lipid was integrated into mER membranes and then complexed with gadolinium. This yielded a potential contrast agent based on mERs.

These different approaches to modification demonstrate the flexibility of mERs and their potential to meet a wide variety of engineering challenges. We believe that additional study can lead to a deeper understanding of controlled release from soft materials, and possibly real world applications in medicine.

Chapter 5

Conclusions

5.1 Project Summary

In this thesis, we have explored a range of different modifications to mERs for applications in therapeutics and diagnostics. We encapsulated glucose oxidase in mERs, allowing the generation of peroxide. These GOx mERs were able to kill cancer cells by glucose starvation and peroxide-activated apoptosis. Microscopy and cell viability measurements allowed us to determine the effectiveness at different GOx concentrations and over time. We extended the release of solutes from mERs by creating an additional barriers to diffusion. This was accomplished with two different approaches, adsorbing chitosan to the surface and encapsulating alginate in the core. We designed a contrast agent by synthesizing a chelator lipid and integrating it into the mER membrane. Complexing with gadolinium yields mERs that should enhance MRI imaging. These studies lay the foundation for many mER applications and provide some new understanding that has not been seen in the literature.

5.2 Recommendations for Future Work

Targeting and Specificity of GOx mERs. We have done some preliminary unpublished work where mERs are modified to target cancer. This was done by incorporating anti-EGFR antibodies into the surface (EGFR is overexpressed in some cancer cells). Further work should further explore targeting capabilities, and quantify their effectiveness. Both data and images should be obtained that can be compared with the work in this thesis. Furthermore, all studies can be replicated with different cancer cell lines as well as healthy cell samples to determine the specificity of the treatment.

Experiments with nano-erythrosomes (nERs). mERs can be reduced to smaller sizes by sonication or extrusion. This reduction may be necessary for actual *in vivo* targeting of cancer cells. Tumors tend to have a leaky vasculature, allowing nano carriers to pass through vessel walls and accumulate.[63]

Animal Studies on GOx mERs. To truly pave the way for human treatment, animal models are necessary to ensure the safety and true effectiveness of new therapies like GOx mERs. Real tumors may respond differently than *in vitro* cancer cells, and toxicity to healthy cells may become a factor. The tumor environment is also distinct and often varies in pH, temperature, and oxygen concentration. Furthermore, immune response may become a concern. Testing GOx mERs *in vivo* would be a major step forward in all aspects.

Colloidal Stability of Chitosan Coated mERs. The chitosan mERs discussed in this thesis tend to cluster rather than remaining fully dispersed. For delivery applications, this can hinder the

viability of the mERs. Further work should explore the mechanism behind this clustering and seek to prevent it from occurring.

Controlled Release Animal Studies. For both chitosan and alginate mERs, it is desired to know if the extending of release reported has a real benefit to the effectiveness of drug delivery. Testing their circulation *in vivo* with some kind of bio-accumulating marker or drug is an important requirement to prove our hypothesis. One possible concept is to use a marker and some modification for targeting and measure the accumulation inside a tumor. The tumor could be excised after the study, and the alginate/chitosan case may show a higher concentration of marker than the control.

MRI with Contrast Agent mERs. The obvious next step is to actually take images using the contrast agent mERs. If they are comparable to existing contrast agent formulations, then the concept is validated. Furthermore, as it stands the preparation of contrast mERs is difficult, and could use improvements to the procedure.

Chapter 6

References

[1] Raghavan, S. R."Liposome." **2016**.

[2] Bangham, A. D. H., R.W. "Negative Staining of Phospholipids and their Structural Modification by Surface-active Agents as observed in the Electron Microscope." **1964**, *8*, 660-668.

[3] Sessa, G. W., G. "Incorporation of Lysozyme into Liposomes." **1970**, *245*, 3295-3301.

[4] Patil, Y. P. J., S. "Novel methods for liposome preparation." **2014**, *177*, 8-18.

[5] Szoka Jr., F. "Comparative Properties and Methods of Preparation of Lipid Vesicles (Liposomes)." **1980**, *9*, 467-508.

[6] Bunker, A. M., A.; Viitala, T. "Rational design of liposomal drug delivery systems, a review: Combined experimental and computational studies of lipidmembranes, liposomes and their PEGylation." **2016**, *1858*, 2334-2352.

[7] Torchilin, V. P. "Recent Advances with Liposomes as Pharmaceutical Carriers." **2005**, *4*, 145-160.

[8] Ponder, E. *Hemolysis and Related Phenomena*; Grune and Stratton, 1948.

[9] Dodge, J. T. M., C.; Hanahan, D.J. "The Preparation and Chemical Characteristics of Hemoglobin-Free Ghosts of Human Erythrocytes." **1962**, *100*, 119-130.

[10] Lesoin, L. C., C.; Boutin, O.; Badens, E. "Preparation of liposomes using the supercritical anti-solvent (SAS) process and comparison with a conventional method." **2011**, *57*, 162-174.

[11] Grit, M. C., D.J.A. "The effect of aging on the physical stability of liposome dispersions." **1992**, *62*, 113-122.

[12] Heurtault, B. S., P.; Pech, B.; Proust, J.E.; Benoit, J.P. "Physio-chemical stability of colloidal lipid particles." **2003**, *24*, 4283-4300.

[13] Cuppoletti, J. M., E.; Zobel, C.R.; Jung, C.Y. "Erythrosomes: Large proteoliposomes derived from crosslinked human erythrocyte cytoskeletons and exogenous lipid." **1981**, *78*, 2786-2790.

[14] Kostic, I. T. I., V.L.; Dordevic, V.B.; Bukara, K.M.; Mojsilovic, S.B.; Nedovic, V.A.; Bugarski, D.S.; Veljovic, D.N.; Misic, D.M.; Bugarski, B.M. "Erythrocyte membranes from slaugherhouse blood as potential drug vehicles: Isolation by gradual hypotonic hemolysis and biochemical and morphological characterization." **2014**, *122*, 250-259.

[15] Kuo, Y. C. Biomimetic Nanostructures for Theranostic Applications, University of Maryland College Park, 2015.

[16] Sabin, J. P., G.; Ruso, J.M.; Hidalgo-Alvarez, R.; Sarmiento, F. "Size and stability of liposomes: A possible role of hydration and osmotic forces." **2006**, *20*, 401-408.

[17] Torchilin, V. P. S., M.I.; Trubetskoy, V.S.; Whiteman, K.; Milstein, A.M. "Amphiphilic vinyl polymers effectively prolong liposome circulation time in vivo." **1994**, *1195*, 181-184.

[18] Sprandel, U. H., A.R.; Chalmers, R.A. "Survival of 'Carrier Erythrocytes' in Dogs." **1980**, *59*, 7P.

[19] Sprandel, U. H., A.R.; Chalmers, R.A. "In Vivo Life Span of Resealed Rabbit Erythrocyte 'Ghosts'." **1980**, *177*, 13-17.

[20] Deak, R. M., J.; Szigyarto, I.C.; Wacha, A.; Lelkes, G.; Bota, A. "Physiochemical characterization of artificial nanoerythrosomes derived from erythrocyte ghost membranes." **2015**, *135*, 225-234.

[21] Kuo, Y. C. W., H.C.; Hoang, D.; Bentley, W.E.; D'Souza, W.D.; Raghavan, S.R. "Colloidal Properties of Nanoerythrosomes Derived from Bovine Red Blood Cells." **2016**, *32*, 171-179.

[22] Gupta, N. P., B.; Nahar, K.; Ahsan, F. "Cell permeable peptide conjugated nanoerythrosomes of fasudil prolong pulmonary arterial vasodilation in PAH rats." **2014**, *88*, 1046-1055.

[23] Hamidi, M. Z., A.; Foroozesh, M.; Mohammadi-Samani, S. "Applications of carrier erythrocytes in delivery of biopharmaceuticals." **2007**, *118*, 145-160.

[24] Favretto, M. E. C., J.C.A.; Bosman, G.J.C.G.M.; Brock, R. "Human erythrocytes as drug carriers: Loading efficiency and side effects of hypotonic dialysis, chlorpromazine treatment and fusion with liposomes." **2013**, *170*, 343-351.

[25] Sprandel, U. H., A.R.; Chalmers, R.A. "Towards Enzyme therapy Using Carrier Erythrocytes." **1981**, *4*, 99-100.

[26] Minsky, M."Microscopy Apparatus." **1961**, *US3013467A*.

[27] Hoare, T. R. K., D.S. “Hydrogels in drug delivery: Progress and challenges.” **2008**, *49*, 1993-2007.

[28] Skoog, D. A. W., D.M.; Holler, F.J.; Crouch, S.R. *Fundamentals of Analytical Chemistry*, 8th ed.; Brooks Cole, 2003.

[29] Caravan, P. E., J.J.; McMurry, T.J.; Lauffer, R.B. “Gadolinium(III) Chelates as MRI Contrast Agents: Structure, Dynamics, and Applications.” **1999**, *99*, 2293-2352.

[30] Schubert, J. “Chelation in Medicine.” **1966**, *214*, 40-51.

[31] Berridge, M. V. H., P.M.; Tan, A.S. “Tetrazolium dyes as tools in cell biology: New insights into their cellular reduction.” **2005**, *11*, 127-152.

[32] Gatti, R. B., S.; Orlandini, G.; Bussolati, O.; Dall’Asta, V.; Gazzola, G.C. “Comparison of Annexin V and Calcein-AM as Early Vital Markers of Apoptosis in Adherent Cells by Confocal Laser Microscopy.” **1998**, *46*, 895-900.

[33] Uggeri, J. G., R.; Belletti, S.; Scandroglio, R.; Corradini, R.; Rotoli, B.M.; Orlandini, G. “Calcein-AM is a detector of intracellular oxidative activity.” **2004**, *122*, 499-505.

[34] Fang, J. S., T.; Maeda, H. “Therapeutic strategies by modulating oxygen stress in cancer and inflammation.” **2009**, *61*, 290-302.

[35] Trachootham, D. A., J.; Huang, P. “Targeting cancer cells by ROS-mediated mechanisms: a radical therapeutic approach?” **2009**, *8*, 579-591.

[36] DiPietrantonio, A. M. H., T.C.; Wu, J.M. “Activation of Caspase 3 in HL-60 Cells Exposed to Hydrogen Peroxide.” **1999**, *255*, 477-482.

[37] Simizu, S. T., M.; Umezawa, K.; Imoto, M. “Requirement of Caspase-3(-like) Protease-mediated Hydrogen Peroxide Production for Apoptosis Induced by Various Anticancer Drugs.” **1998**, *273*, 26900-26907.

[38] Yuan, J. S., S.; Ledoux, S.; Ellis, H.M.; Horvitz, H.R. “The C. elegans Cell Death Gene *ced-3* Encodes a Protein Similar to Mammalian Interleukin-1β-Converting Enzyme.” **1993**, *75*, 641-652.

[39] Warburg, O. W., F.; Negelein, E. “The Metabolism of Tumors in the Body.” **1927**, *8*, 519-530.

[40] Cheng, J. L., Q.; Shuhendler, A.J.; Rauth, A.M.; Wu, X.Y. “Optimizing the design and in vitro evaluation of bioreactive glucose oxidase-microspheres for enhanced cytotoxicity against multidrug resistant breast cancer cells.” **2015**, *130*, 164-172.

[41] Huo, M. W., L.; Chen, Y.; Shi, J. “Tumor-selective catalytic nanomedicine by nanocatalyst delivery.” **2017**, *8*, 1-12.

[42] Li, J. L., Y.; Wang, Y.; Ke, W.; Chen, W.; Wang, W.; Ge, Z. “Polymer Prodrug-Based Nanoreactors Activated by Tumor Acidity for Orchestrated Oxidation/Chemotherapy.” **2017**.

[43] Zhao, W. H., J.; Gao, W. “Glucose Oxidase-Polymer Nanogels for Synergistic Cancer-Starving and Oxidation Therapy.” **2017**, *9*, 23528-23535.

[44] Yamaguchi, Y. S., M.; Stanislawski, L.; Strosberg, A.D.; Stanislawski, M. “Virucidal Effects of Glucose Oxidase and Peroxidase or Their Protein Conjugates on Human Immunodeficiency Virus Type 1.” **1993**, *37*, 26-31.

[45] Casentini-Borocz, D. B., T. “Enzyme Immunoconjugates Utilizing Glucose Oxidase and Myeloperoxidase Are Cytotoxic to Candida tropicalis.” **1990**, *34*, 875-880.

[46] Cai, Y. L., J.; Miao, Z.; Lin, L.; Ding, J. “Reactive Oxygen Species Contribute to Cell Killing and P-Glycoprotein Downregulation by Salvicine in Multidrug Resistant K562/A02 Cells.” **2007**, *6*, 1794-1779.

[47] Agostinelli, E. T., G.; Viceconte, N.; Saccoccio, S.; Battaglia, V.; Grancara, S.; Toninello, A.; Stevanato, R. “Potential anticancer application of polyamine oxidation products formed by amine oxidase: a new therapeutic approach.” **2010**, *38*, 353-368.

[48] Seeman, P. C., D.; Iles, G.H. “Structure of the Membrane Holes in Osmotic and Saponin Hemolysis.” **1973**, *56*, 519-527.

[49] Pajic-Lijakovic, I. “Role of band 3 in the erythrocyte membrane structural changes under thermal fluctuations –multi scale modeling considerations.” **2015**, *47*, 507-518.

[50] Pajic-Lijakovic, I. I., V.; Bugarski, B.; Palvsic, M. “Rearrangement of erythrocyte band 3 molecules and reversible formation of osmotic holes under hypotonic conditions.” **2010**, *39*, 789-800.

[51] Salhany, J. M. C., K.A.; Sloan, R.L. “Mechanism of band 3 dimer dissociation during incubation of erythrocyte membranes at 37 C.” **2000**, *345*, 33-41.

[52] Sato, Y. Y., H.; Suzuki, Y. “Mechanism of hypotonic hemolysis of human erythrocytes.” **1993**, *16*, 506-512.

[53] Cribier, S. M., G.; Neumann, J.M.; Devaux, P.F. “Lateral diffusion of erythrocyte phospholipids in model membranes comparison between inner and outer leaflet components.”

[54] Schrier, S. L. Z., A.; Herve, P.; Kader, J.C.; Devaux, P.F. “Transmembrane redistribution of phospholipids of the human red cell membrane during hypotonic hemolysis.” **1992**, *1105*, 170-176.

[55] Haest, C. W. M. P., G.; Kamp, D.; Deuticke, B. “Spectrin as a Stabilizer of the Phospholipid Asymmetry in the Human Erythrocyte Membrane.” **1978**, *509*, 21-32.

[56] Pajic-Lijakovic, I. M., M. “Modeling analysis of the lipid bilayer–cytoskeleton coupling in erythrocyte membrane.” **2014**, *13*, 1097-1104.

[57] Steck, T. L. K., J.A. “Preparation of Impermeable Ghosts and Inside-out Vesicles from Human Erythrocyte Membranes.” **1974**, *31*, 172-180.

[58] Hardy, B. S., S.L. “The Role of Spectrin in Erythrocyte Ghost Endocytosis.” **1978**, *81*, 1153-1161.

[59] Liu, X. L., Y.P.; Zhong, Z.M.; Tan, H.Q.; Lin, H.P.; Chen, S.J.; Fu, Y.C.; Xu, W.C.; Wei, C.J. “Incorporation of Viral Glycoprotein VSV-G Improves the Delivery of DNA by Erythrocyte Ghost into Cells Refractory to Conventional Transfection.” **2017**, *181*, 748-761.

[60] Johnson, R. M. “The Kinetics of Resealing of Washed Erythrocyte Ghosts.” **1975**, *22*, 231-253.

[61] Li, X. X., A.; Xie, H.; Yu, W.; Xie, W.; Ma, X. “Preparation of low molecular weight alginate by hydrogen peroxide depolymerization for tissue engineering.” **2010**, *79*, 660-664.

[62] Jasanada, F. U., P.; Souchard, J.P.; Le Gaillard, F.; Favre, G.; Nepveu, F. “Indium-111 Labeling of Low Density Lipoproteins with the DTPA-Bis(stearylamide): Evaluation as a Potential Radiopharmaceutical for Tumor Localization.” **1996**, *7*, 72-81.

[63] Danhier, F. F., O.; Préat, V. “To exploit the tumor microenvironment: Passive and active tumor targeting of nanocarriers for anti-cancer drug delivery.” **2010**, *148*, 135-146.